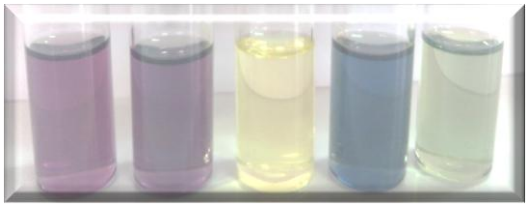

CHAPTER VI

Synthesis, characterization and study of new 1,3,5-tris[4-{(2-hydroxyarylidene)-amino-/aminophenyl-4-oxy}-methyl]-2,4,6-trimethylbenzenes

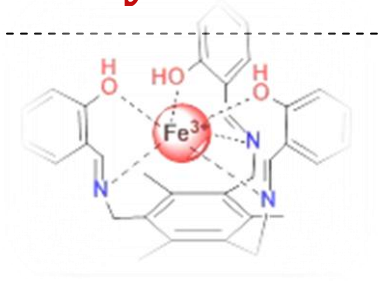

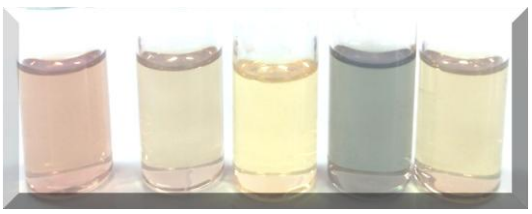

6.1 INTRODUCTION

A primary amine and an aldehyde or a ketone undergo nucleophilic condensation reaction to give the compound with >C=N– functionality which is called an *imino* functionality and the compounds containing imino functionality are known as imines. The imines are also known as Schiff bases[1] named after a Jewish chemist Professor Hugo Joseph Schiff. >C=N linkage is also known as azomethine linkage. Aldehydes are more reactive compared to ketones with similar substituents attached to the carbonyl group. Aromatic aldehydes with electron withdrawing substituents are more reactive compared to the aldehydes with electron releasing substituents.

Imine functionality is an important useful functionality which can undergo various addition or cycloaddition (may not be concerted) [2] reactions leading to the corresponding amino compounds or nitrogen containing heterocyclic compounds. Many important heterocycles such as pyrroles,[3] imidazoles, thiazolidinones, pyridines, lactams have been reported for their synthesis from imino compounds with different synthesis approaches.

A one-pot cycloaddition reaction of α,β-unsaturated imino compounds with internal alkynes resulted in the six member nitrogen containing pyridine heterocyclic compounds **1**[4] (Figure 1).

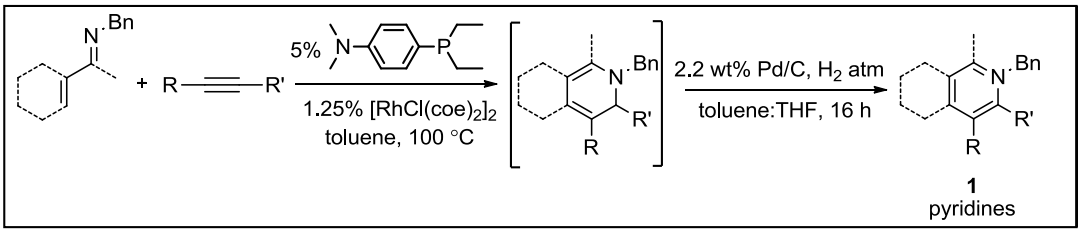

Figure 1 ***Application of imines in synthesis of pyridines***

In an another reaction imino compounds on reaction with acid chlorides and alkynes led to highly substituted pyrroles **2**[5] (Figure 2).

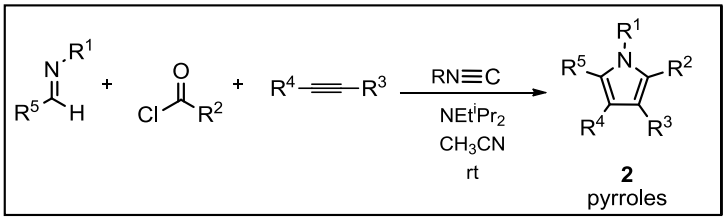

Figure 2 ***Pyrroles from imines***

Staudinger reaction of imines and ketenes lead to a highly enantioselective synthesis of *N*-Boc *β*-Lactams **3**[6] (Figure 3).

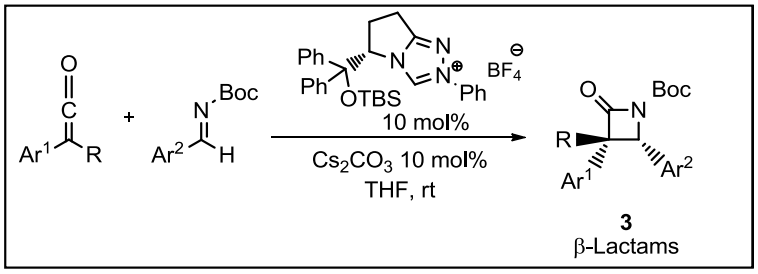

Figure 3 ***Imines to enantioselective β-Lactams***

A multicomponent palladium catalyzed coupling of imino compounds and acid chloride provided an efficient methodology for the synthesis of the imidazole heterocycle compounds **4**[7] (Figure 4).

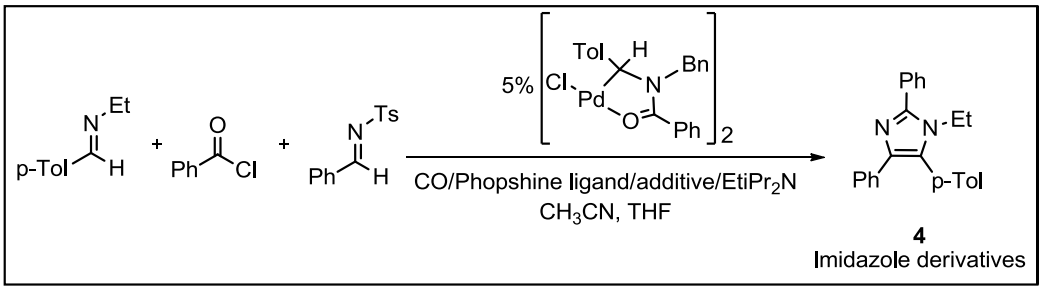

Figure 4 ***Synthesis of imidazoles***

An efficient and asymmetric preparation of amines was achieved by catalytic enantioselective addition reactions to imino compounds[8] as included in the following reactions.

The reaction of benzhydrylimines with hydrogen cyanide gave α-aminonitriles **5** in asymmetric Strecker's synthesis[9] (Figure 5).

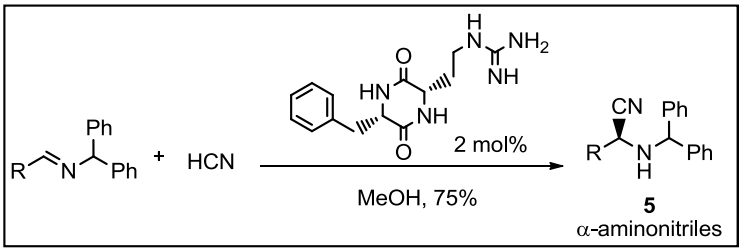

Figure 5 ***Aminonitriles from benzhydrylimines***

Enantioselective synthesis of arylamines **6** was reported by of addition of imines[10] (Figure 6).

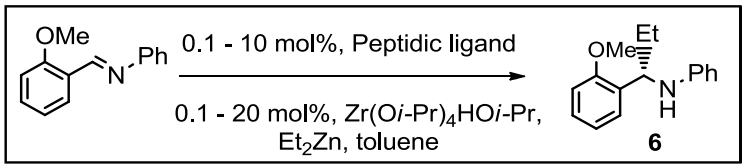

Figure 6 ***Enantioselective addition to imines***

Imines offer a binding site through its nitrogen atom for complexation with metal ions along with an additional complementary site present which make them efficient chelating ligands[11] (Figure 7).

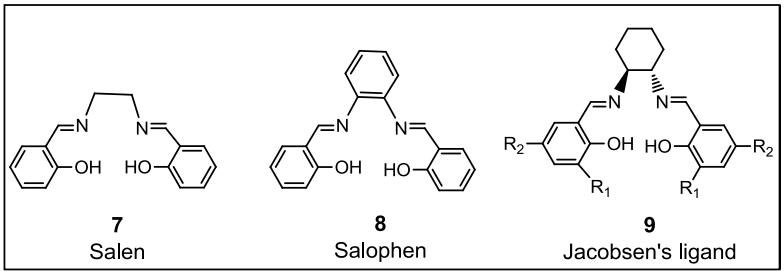

Figure 7 ***Widely used salen ligands***

They have an ability to bind strongly with metal ions thus they are useful in many applications. Metal complexes imino ligands also act as efficient catalysts for various reactions.[12]

As an example, titanium complex of chiral salen ligand was found to catalyze pinacol coupling reaction of aryl aldehydes by *in situ* reduction of Ti(IV) complexes with zinc[13] (Figure 8).

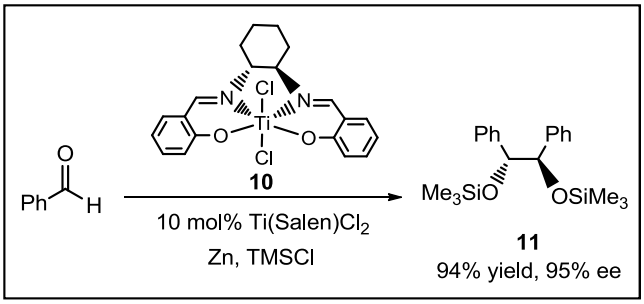

Figure 8 ***Catalytic enantioselective coupling of aldehydes***

Schiff bases or imines are not only evergreen chemistry tools[1] but are also biologically important compounds. Schiff bases are versatile pharmacophores which exhibit various biological activities such as antimicrobial activity,[14] antifungal, antituberculer activity, antitumor activity,[15] anti-inflammatory activity,[16] antidepressant activity and

anticonvulsant activity to count a few[1] (Figure 9). Some recent reviews on the subject carry detailed information on various biological activities mentioned of these compounds.[17]

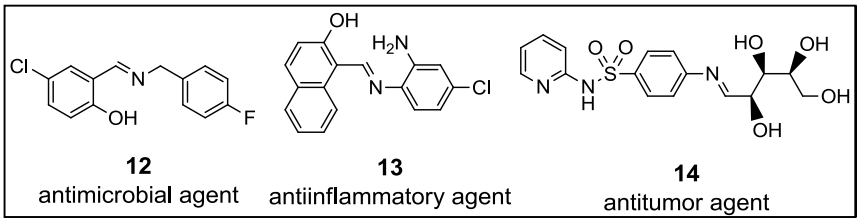

Figure 9 ***Bioactive imines***

6.1.1 Tripodal imino compounds

Recently, there has been a lot of interest generated in the synthesis of C_3 symmetric compounds having imine linked podands. The tripodal tris-imines have been prepared mainly from tris-amines such as tris-aminoethylamine (TREN)[18] (Figure 10) or tris-aminomethylcyclohexane[19] (Figure 11).

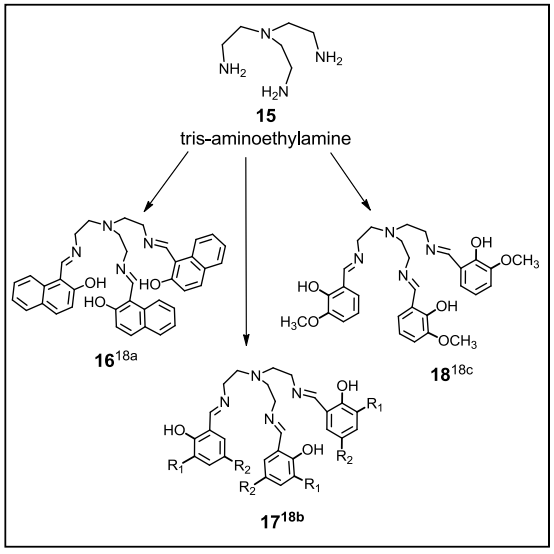

Figure 10 ***TREN derived tripodal imines***

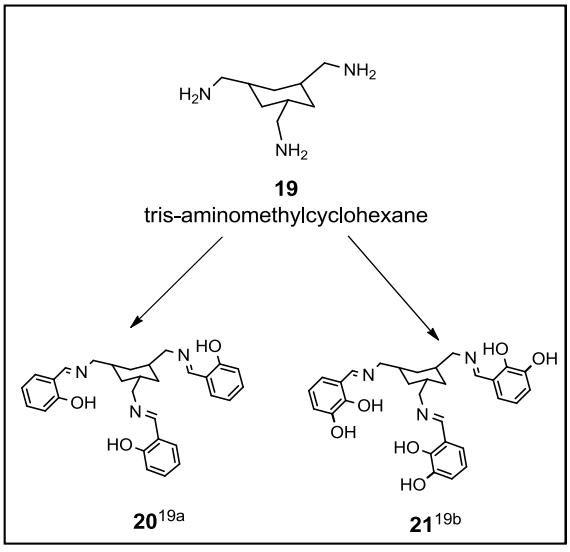

Figure 11 ***Tris-aminomethyl cyclohexane derived tripodal imines***

The other tris-amino compounds employed for the imine synthesis have been prepared by attaching mono amines to a C_3 symmetric linker giving higher generation tris-amines. Almost all of the imines thus prepared are desired to possess *ortho* hydroxyl group offering tripodal salen chelating sites which have been extensively used for recognition of various metal ions. Tripodal compounds with chelating ability can bind to a metal ion

more tightly with the involvement of multiple binding sites and can have specific recognition ability.

Various *ortho*-hydroxyimino compounds have been reported by condensation of salicaldehyde derivatives with tris-aromatic amine.[20] One such tripodal tris-imino compound **22** (Figure 12) was found to recognize Cu^{2+} ions in aqueous medium.[21]

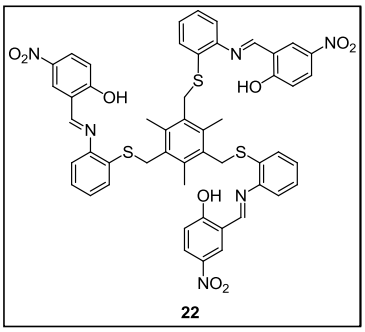

Figure 12 ***Tripodal Cu^{2+} sensor***

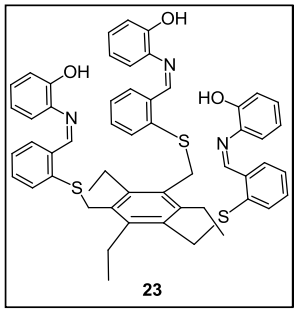

Figure 13 ***Tris-imino Ag^{+} sensor***

Closely related tripodal receptor **23** found to recognize Ag^{+} ions in aqueous medium with enhancement of fluorescence[22] (Figure 13). Similar azo coupled chromogenic tripodal receptor **24** had capability of visual detection of Ag^{+} ions in aqueous medium[23] (Figure 14).

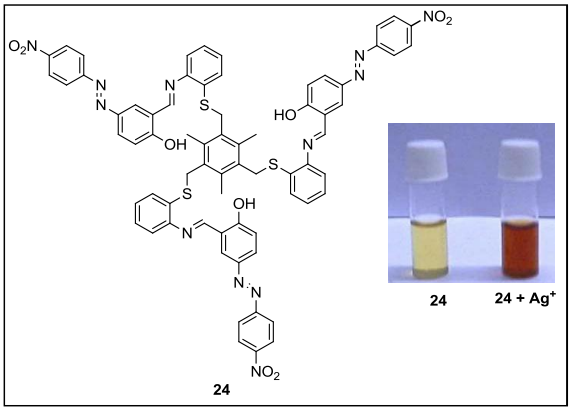

Figure 14 ***Tripodal chromogenic sensor for Ag^{+}***

A number of reports comprising the synthesis of tris-imines having *ortho*-hydroxy substituents and their applications in selective recognition of a guest entity, directed the present project on C_3 symmetric compounds towards the synthesis of new such tris-imino host molecules.

6.2 RESULTS AND DISCUSSION

In the present chapter, which deals with the synthesis of new host molecules- two types of amino compounds have been prepared and employed for imine synthesis. One is a tris-benzyl amine namely 1,3,5-trisaminomethyl-2,4,6-trimethylbenzene which is a tris-aliphatic amine and the other is tris-aromatic amine namely 1,3,5-tris-(4-aminophenoxymethyl)-2,4,6-trimethylbenzene.

Tris-aminomethyl mesitylene derivative **27** was prepared from the common C_3 symmetry inducing starting material employed in this thesis namely tris-bromomethyl mesitylene **25** which was converted the corresponding tris-azide **26** by reacting with sodium azide in DMF nearly in quantitative yield (Scheme 6.1).[24] The tris-azide **26** was transformed in to the tris-amine **27** by reducing with hydrogen in presence of Pd/C in an overnight reaction in an excellent yield.[25] (Scheme 6.1)

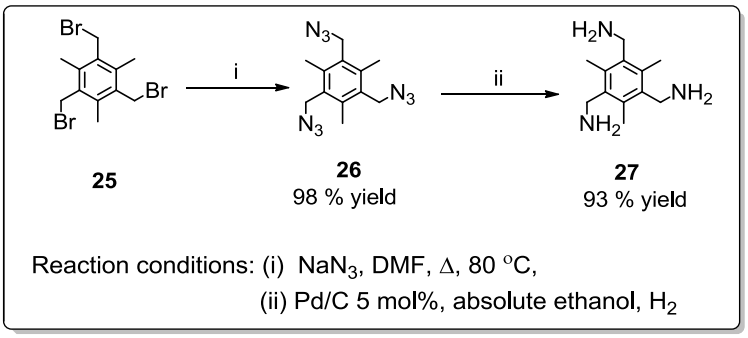

Scheme 6.1 ***Synthesis of tris-aminomethyl mesitylene 25***

Condensation of this tris-amine **27** with salicaldehyde and its derivatives **28** such as 5-bromo salicaldehyde, 5-nitro salicaldehyde and *o*-vanillin as well as with 2–hydroxy–1–napthaldehdye lead to promising C_3 symmetric host molecules **29** with three salen chelating sites in good yields (Scheme 6.2).

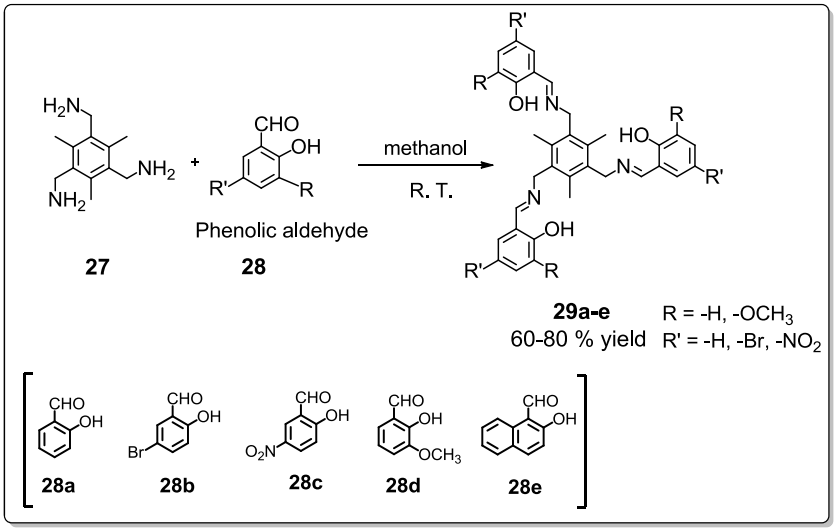

Scheme 6.2 ***Triple condensation to imines***

In infrared spectra of the tris-imines **29**, a medium intensity broad band is observed between 3400 to 3450 cm^{-1} for ν_{O-H}. A strong band around 1630 cm^{-1} for $\nu_{C=N}$. The $\nu_{C=C}$ for aromatic rings are observed with varying intensities between 1600 to 1470 cm^{-1}. A strong band ~ 1280 cm^{-1} is assigned for ν_{Ar-O}. The compound **29d** with methylether linkage ($-OCH_3$) is having additional bands for C–O stretching at 1079 and 1050 cm^{-1} (Spectrum 17).

^{1}H NMR spectra of these compounds had typical signals at δ 2.4 for central ring attached methyl group protons and a singlet near δ 5.0 for $-NCH_2$ group protons attached to the same ring. A singlet between δ 8.2 to 8.8 was assigned for the protons attached to the imine carbon and a singlet between δ 13.5 to 15.0 was due to phenolic –OH group protons. In the *o*-vanillin derived tris-imino compound **29d** methoxy protons signals are observed at δ 3.90 (Spectrum 18). The signals for aromatic protons are observed as per the substitution pattern.

In ^{13}C-NMR spectra the most downfield carbon is observed between δ 163 to 174 for the hydroxyl (Ar-OH) attached aromatic carbon which is accompanied by imine carbon (–C=N) falling in between δ 151 to 166. The aromatic carbons are observed between δ 107 and 140 while bromine attached carbon signal is observed at δ 96.0 and methoxy ($-OCH_3$) carbon signal is seen at δ 56.1. Methyl group carbon signal is observed at δ 16.3 or 16.6 while methylene carbon ($-NCH_2$) signal is observed from δ 52.0 to 56.3.

The tris-imines were also characterized by the mass analysis with TOF mass analyzer with electron spray technique. The molecular ion peaks for all the tripodal compounds corresponds to $(M+Na)^+$ except for compound **29b** (–Br substituted; Spectrum 12) and compound **29c** (–NO_2 substituted; Spectrum 32).

6.2.1 Host-guest binding study

Host-guest binding study of C_3 symmetric tripodal imino compounds was carried out with first row transition metal ions in DMSO as a solvent. DMSO is considered to be a biocompatible solvent which is advantageous for such studies in biological systems. UV-Visible spectroscopy and fluorescence spectroscopy both were used to detect host-guest interactions. Metal ion solutions were prepared as their perchlorate salts with ten times higher concentration than that of the synthesized host compounds as follows.

[Host] = 3.2×10^{-4} M for **29 (a, d, e)** and [Host] = 5.5×10^{-4}M for **29b, 29c**
[Guest] = 3.2×10^{-3} M **29 (a, d, e)** and [Guest] = 5.5×10^{-3} M for **29b, 29c**

The UV-Vis spectrum of **29a** is having two absorption bands in the region 300 to 500 nm (Figure 15, Graph 2). Host-guest interactions were studied by mixing an equal volume of above prepared solutions of hosts and metal perchlorate salts as guests and their UV-Vis spectra were recorded. There was no significant change in λ_{max} in the presence of Mn^{2+}, Co^{2+}, Ni^{2+} and Zn^{2+}. There was a clear shift in λ_{max} in the presence of Cu^{2+} ions without change in absorbance (Figure 15, Graph 1). In the presence of Fe^{3+} ions, a new band emerged at λ_{max} 539 nm which was visibly seen with the development of magenta coloured solution (Figure 15, Graph 1 and inset) in addition to a large shift in absorption band with increased absorbance. Thus the host compound **29a** was found to be a colorimetric sensor for Fe^{3+}. A selectivity study for Fe^{3+} ion was carried out in presence of the other metal ions studied. It was found that the host selectively binds with the Fe^{3+} ions even in presence of the other metal ions (Figure 15, Graph 2).

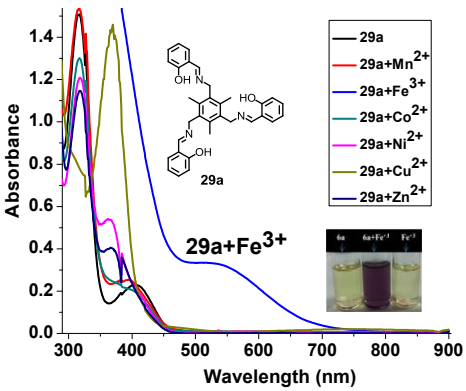

Graph 1: UV-Vis spectra

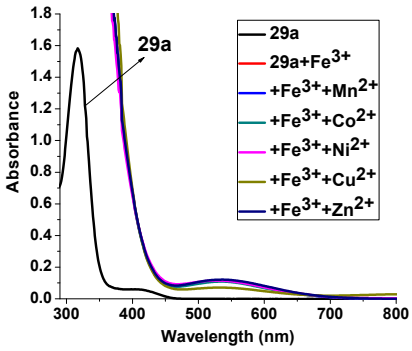

Graph 2: Fe^{3+} selectivity study in UV-Vis spectra

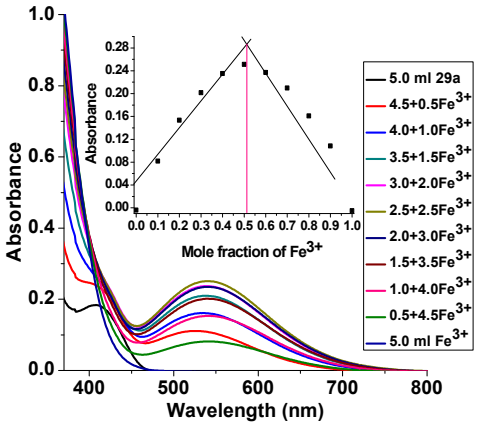

Graph 3. Job's plot of 29a at λ = 539 nm

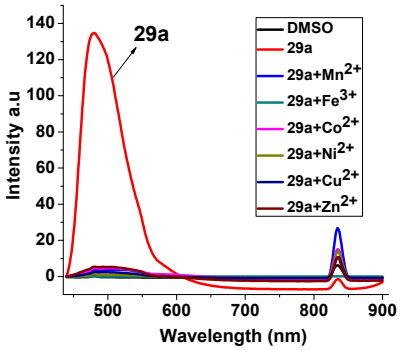

Graph 4. Fluorescence spectra at λ_{ex}= 420 nm

Figure 15 ***Host-guest study of compound 29a with I series transition metal ions***

To know the binding ratio between the host and guest entities, Job's method was employed with changing host:guest concentration and observed the changes taking place at λ = 539 nm (Figuer 15, Graph 3 and inset). The result showed that, though there are three chelating sites in the tripodal host molecule, only one Fe^{3+} ion is accommodated in the tripod as depicted in the figure (Figure 16).

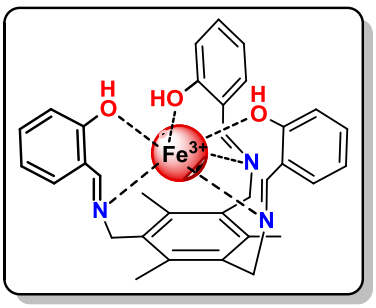

Figure 16 ***Binding of compound 29a with*** Fe^{3+}

Photoluminescence study showed that the host molecule **29a** was fluorescent when excited at λ 420 nm with an emission band at λ 479 nm. The binding study carried out using fluorescence spectroscopy showed that on addition of any of the transition metal ions under study, the fluorescence observed for the host molecule was quenched (Figure 15, Graph 4). These results indicated that all the metal ions studied were bound with the host molecules which was not clearly observable with the help of UV-Vis spectroscopy. As all the metal ions switch off the fluorescence, the selectivity study was not carried out.

The bromo substituted host molecule **29b** showed a similar behavior with that of the host **29a** without Br substitution. The UV-Vis study conducted for **29b** also showed an emergence of a new absorption band at λ 517 nm in the presence of Fe^{3+} ions which was even visibly observed by the distinct colour change of the host solution upon addition of the Fe^{3+} ions (Figure 17, Graph 5 and inset). The selectivity study of the host molecule with other transition metal ions showed that the host is selective for Fe^{3+} except in presence of Cu^{2+} which lowers the absorbance compared to that in presence of Fe^{3+}. Thus there was a little interference of Cu^{2+} ions in binding of Fe^{3+} ions in this case (Figure 17, Graph 6). The Job's plot indicated 1:1 host-guest binding ratio similar to the earlier host compound (Figure 17, Graph 18).

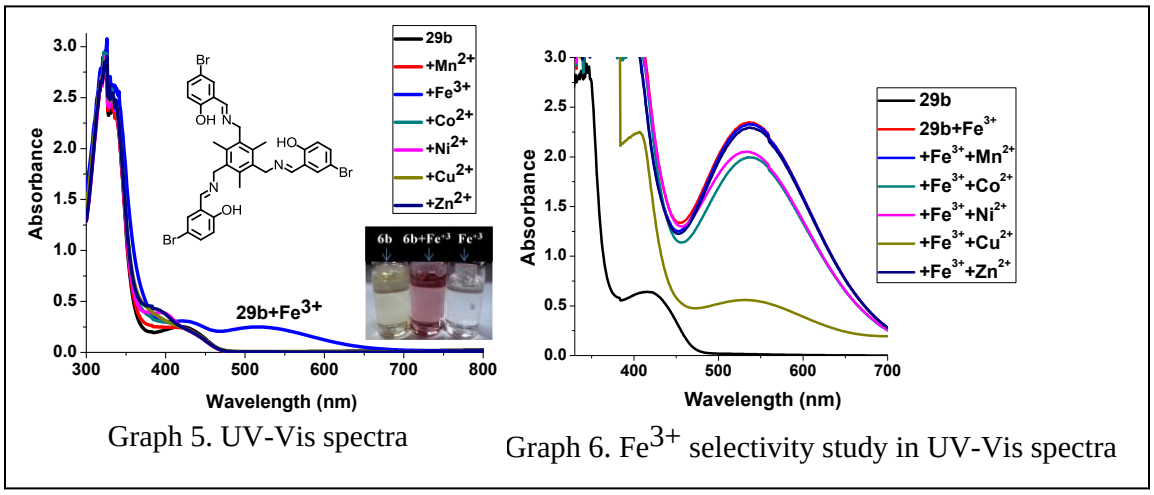

Graph 5. UV-Vis spectra

Graph 6. Fe^{3+} selectivity study in UV-Vis spectra

Figure 17 ***Host-guest study of compound 29b with I series transition metal ions***

continued...

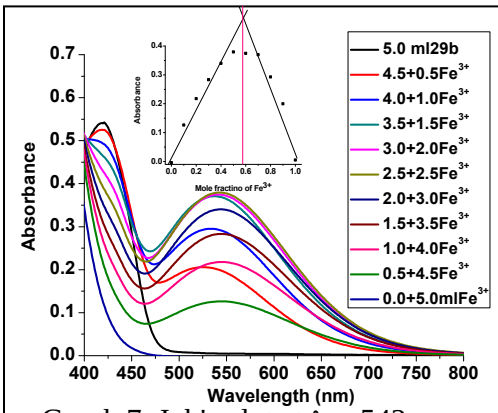

Graph 7. Job's plot at λ = 542 nm

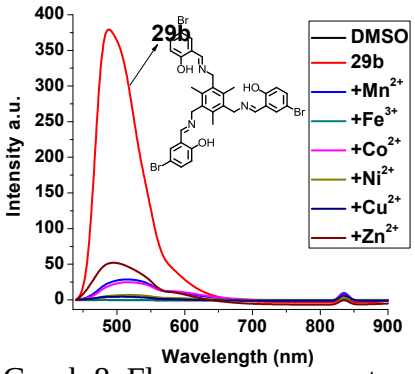

Graph 8. Fluorescence spectra at λ_{max}= 420 nm

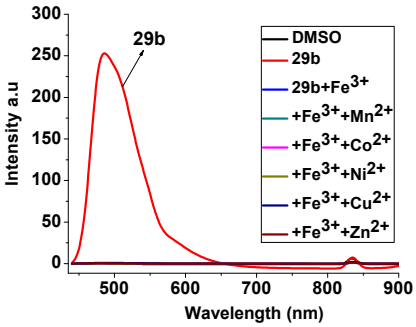

Graph 9. Fe^{3+} selectivity study in fluorescence spectra

Figure 17 ***Host-guest study of compound 29b with I series transition metal ions***

The tripodal bromo compound **29b** showed photoluminescence when excited at λ 420 nm with a strong emission at λ 488 nm (intensity of 380). The fluorescence of **29b** was reduced considerably or getting off in the presence of transition metal ions studied (Figure 17, Graph 8). The fluorescence study was also carried out to test the selectivity of Fe^{3+} ions which showed complete quenching of the fluorescence in the presence of Fe^{3+} along with the other metal ions in the solution (Figure 17, Graph 9). Thus selective recognition of the host molecule was endorsed by the fluorescence study.

The other two tripodal host compounds, **29c** and **29d** possessing nitro and methoxy substitutions respectively showed their binding ability with the transition metal ions under study as can be observed from their UV-vis spectra presented in the respective figures (Figure 18, Graph 10, 11 and inset figures). There was a distinct colour change of the host solution **29d** from pale yellow to dark bluish-green in the presence of Fe^{3+} ions (Figure 18, Graph 11; inset).

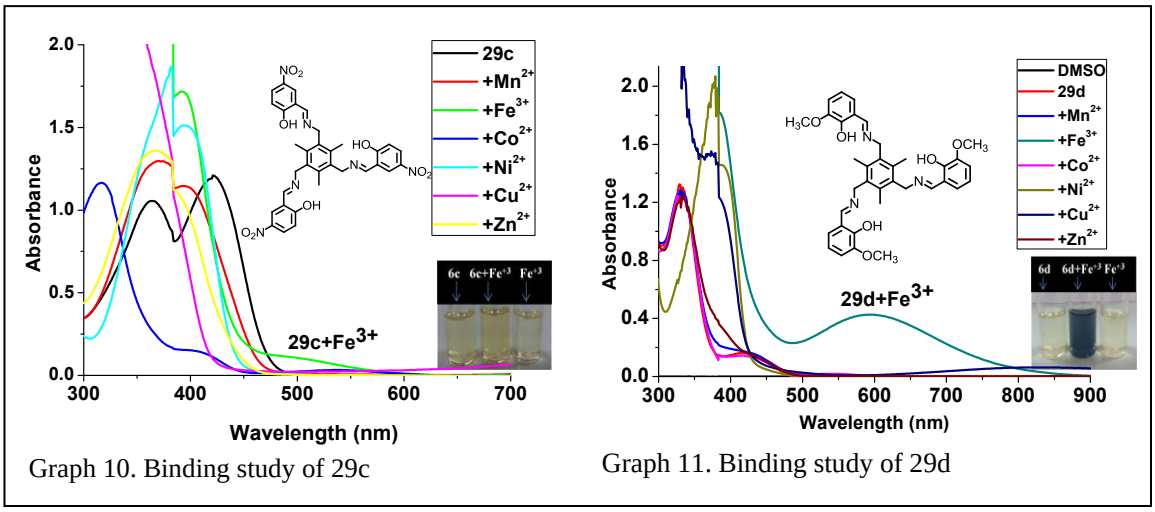

Graph 10. Binding study of 29c

Graph 11. Binding study of 29d

Figure 18 ***Host-guest study of 29c and 29d with transition metal ions***

Job's plot study showed that the binding stoichiometry of host : guest to be 1:2 for nitro substituted tripodal host 29c (Figure 19, Graph 12) unlike methoxy substituted host compound 29d having 1:1 host-guest binding ratio (Figure 19, Graph 13).

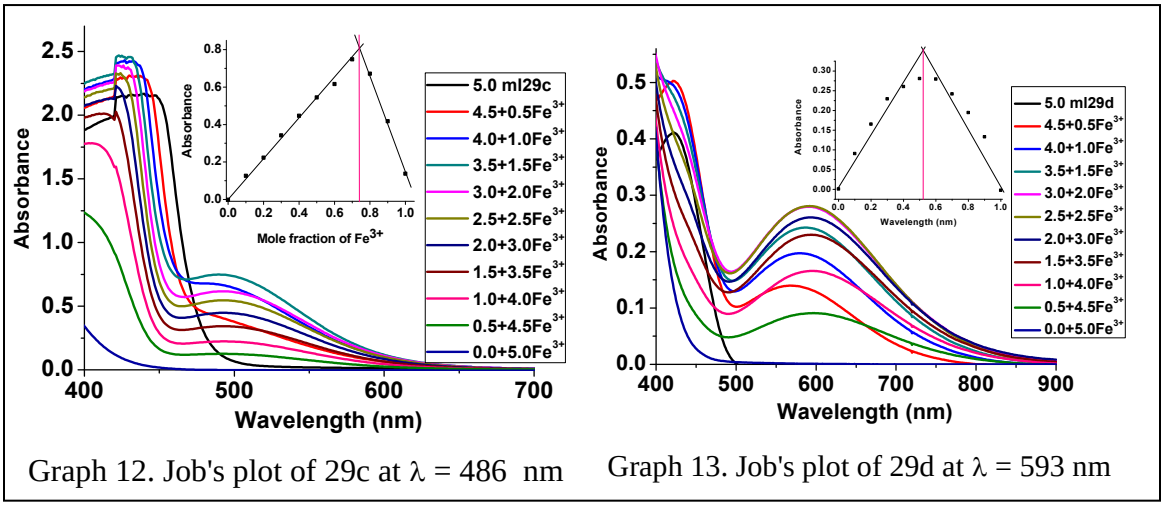

Graph 12. Job's plot of 29c at λ = 486 nm

Graph 13. Job's plot of 29d at λ = 593 nm

Figure 19 ***Job's plot of 29c and 29d***

The selectivity of Fe^{3+} binding using UV-Vis spectroscopy for compound **29c** having nitro substituent showed that the host does not bind with all the guests ions in presence of Fe^{3+} ions but has the interference of other guest ions like Co^{2+}, Ni^{2+} and Cu^{2+} ions (Figure 20, Graph 14). The host compound with methoxy substitution **29d** showed good selectivity for Fe^{3+} ions in the presence of the other guest ions and hence found to be a better host for Fe^{3+} binding (Figure 20, Graph 15).

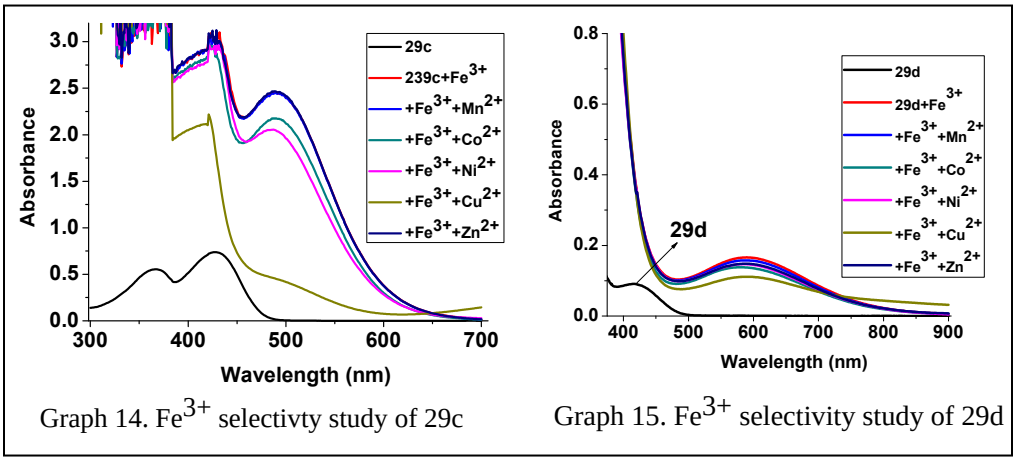

Graph 14. Fe^{3+} selectivty study of 29c

Graph 15. Fe^{3+} selectivity study of 29d

Figure 20 ***Selectivity study of compounds 29c and 29d using UV-Vis spectroscopy***

Photoluminescence study of **29c** (with nitro substitution) showed that all the guest ions do not quench the fluorescence to very low values as observed for other hosts but Fe^{3+} quenched the fluorescence completely (Figure 21, Graph 16). The Fe^{3+} was found to completely quench the fluorescence even in the presence of the other metal ions (Figure 21, Graph 17).

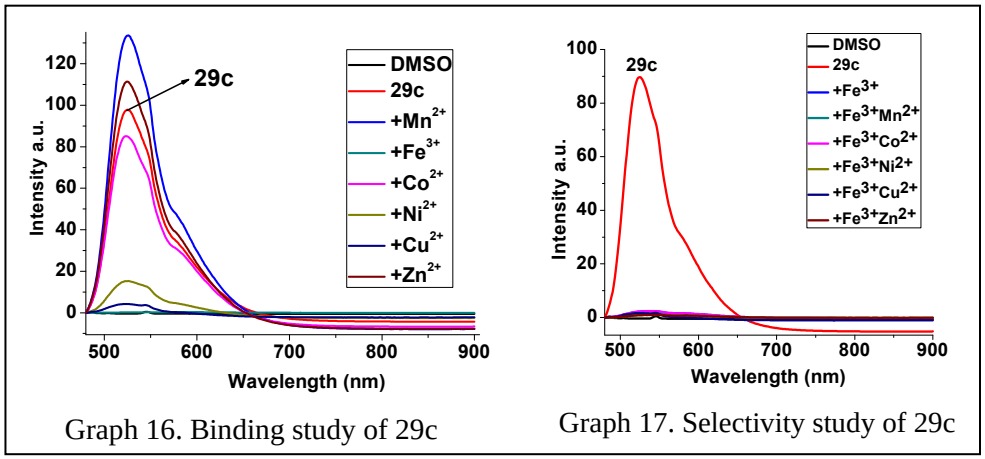

Graph 16. Binding study of 29c

Graph 17. Selectivity study of 29c

Figure 21 ***Binding study of compound 29c using fluorescence***

The selectivity of Fe^{3+} binding was well observed in UV-Vis (Figure 20, Graph 15) and fluorescence studies for the host **29d** with methoxy substitution (Figure 22, Graph 18 and 19).

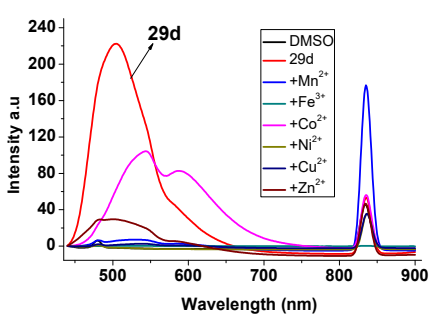

Graph 18. Binding study of 29d

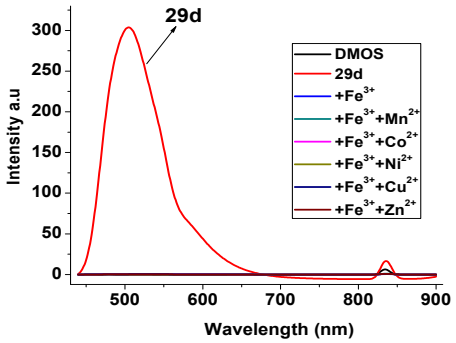

Graph 19. Fe^{3+} selectivity study

Figure 22 ***Binding study of compound 29d using fluorescence***

The tripodal host **29e** with the change in aromatic moiety from phenyl to napthyl, still distinctly recognized Fe^{3+} ions with the same 1:1 host to guest stoichiometry as studied with the help of Job's plot.

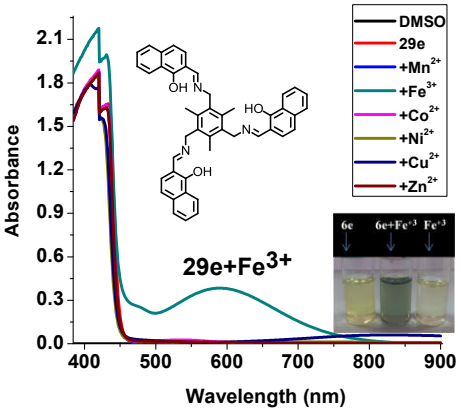

Graph 20. UV-Vis spectra for binding study

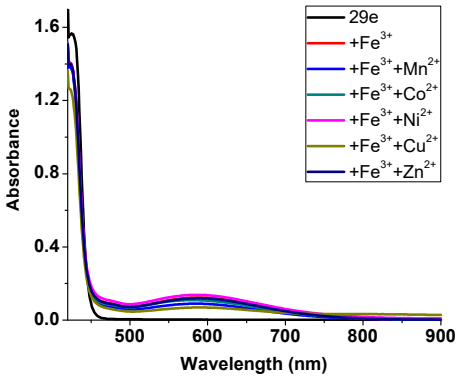

Graph 21. UV-Vis spectra for Fe^{3+} selectivity

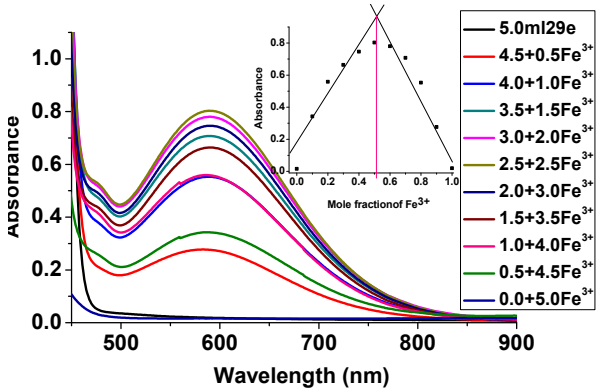

Graph 22. Job's plot at λ = 591 nm

Figure 23 ***Binding study using UV-vis and Job's plot of compound 29e***

Compound **29e** was found to be non-fluorescent in nature thus restricting binding study using UV-vis spectroscopy (Figure 23).

6.2.2 Synthesis and study of remotely placed tris-imino functionalities

The imines derived from 1,3,5–trisaminomethyl–2,4,6–trimethylbenzene **29** had the binding sites oriented near the central linker phenyl ring and they were found to co-ordinate with one guest entity with complementary orientation. In continuation with this work, it was planned to place the imino functionalities at a distant position compared to the earlier synthesized C_3 symmetric tripodal imines retaining the symmetry element. Thus a phenyl ring was placed in between the central aromatic moiety and imino functionalities.

With this aim, 1,3,5–tris(4–aminophenyloxymethyl)–2,4,6–trimethylbenzene was prepared by coupling of 4-nitrophenol with tris-bromo mesitylene **25** under usual Williamson's synthesis condition (K_2CO_3, acetone)[26] resulting in a C_3 symmetric tri-nitrophenyloxy derivative **30**. The tris-nitro compound was reduced to 1,3,5–tris(4–aminophenyloxymethyl)–2,4,6–trimethylbenzene **31** following the reported methodology (Scheme 6.3).[26]

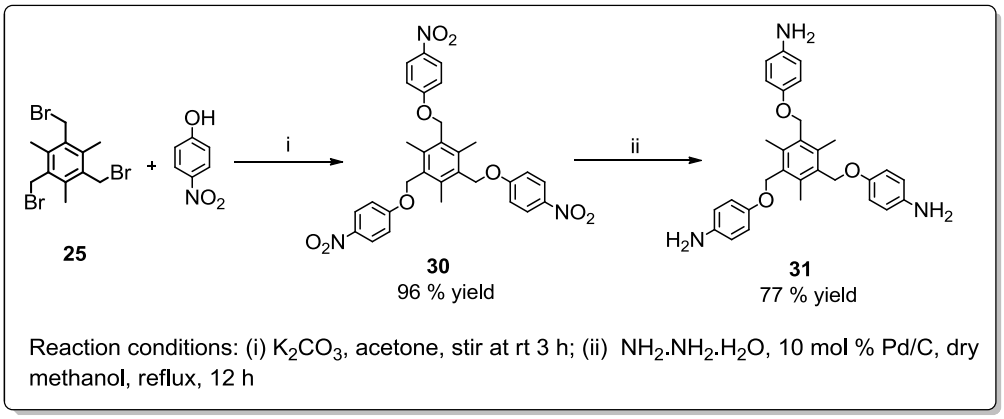

Scheme 6.3

The C_3 symmetric tris-aromatic amine **31** was condensed with five different phenolic aldehydes by refluxing in methanol in good yields. The resulting tris-imino *ortho*–hydroxy binding sites in these tripodal compounds **32** are situated farther from the central aromatic ring (Scheme 6.4).

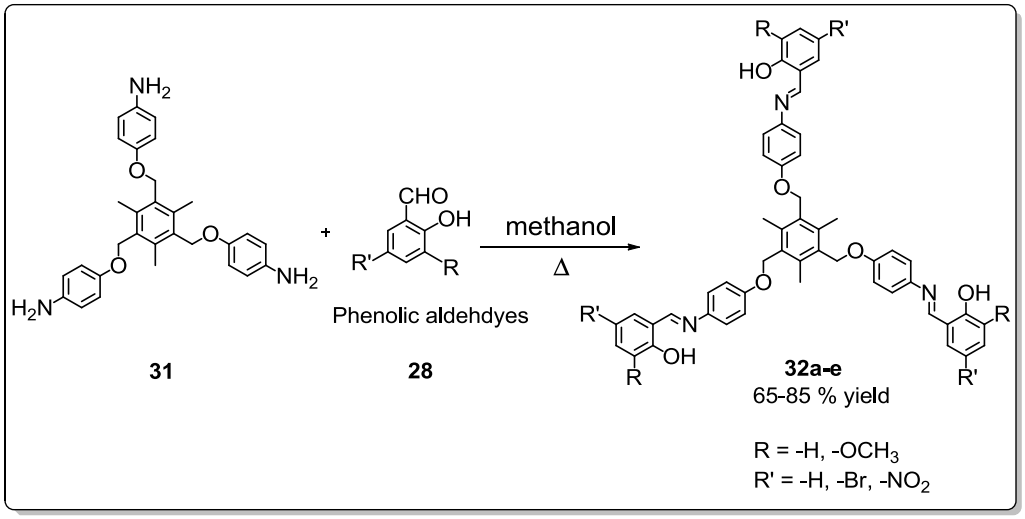

Scheme 6.4

The tripodal imine **32e** having 2-hydroxy naphthyl end groups was recently reported in literature as selective fluorescent sensor for Al^{3+} and Pb^{2+} ions.[26] The newly prepared tripodal compounds were characterized by using various spectroscopic techniques.

The IR spectra of the tris-imines **32**, showed a band at 3435 cm^{-1} for ν_{O-H} in most cases. The imino $\nu_{C=N}$ was shifted to a lower value at 1616 cm^{-1} than that of the earlier analogous imine. Aromatic $\nu_{C=C}$ were observed between 1600 (hump) to 1450 cm^{-1}. The ν_{Ar-O} were observed at 1280, 1235 and 1080-1110 cm^{-1} including ν_{C-O} of $-OCH_3$ in compound **32d** (Spectrum 37).

^{1}H NMR spectra of these compounds show a singlet for protons of $-CH_3$ group on the central aromatic ring at δ 2.5 and a singlet for the oxygen attached methylene group ($ArOCH_2$) protons at δ 5.17. Imine carbon attached proton (–N=CH–) is observed as a singlet at δ 8.6 except for nitro substituted compound where it is observed as downfield as δ 9.17. While hydroxyl proton (–OH) singlet is observed between δ 13.4 to 13.9. The compound with methoxy substitution **32e** is characterized by a singlet for $-OCH_3$ at δ 3.96 (Spectrum 42). The aromatic proton signals are well separated for tripodal compound possessing bromo and nitro groups (Spectrum 30 & 34). In the nitro substituted tris-imine **32c**, one of the aromatic proton signal is observed as downfield as 8.64 as a doublet with J = 2.8 Hz (meta coupling) (Spectrum 34). All the compounds are

also characterized by the presence of typical two doublets for the para substituted aromatic ring at δ 7.1 and 7.35 due to protons on the aromatic linker ring.

In ^{13}C-NMR, the downfield ^{13}C signals very close to each other are for aromatic carbons attached to hydroxyl group (Ar-OH) followed by carbon of the imine linkage (–C=N) and aromatic carbons for arylmethylene ether (ArO-CH_2). The methylidene carbon is always observed between the two oxygen attached aromatic carbons which was clearly apparent from DEPT results. The other aromatic carbons are observed mostly between δ 110 to 151. The bromo attached aromatic carbon signal was observed at δ 96.1. The aromatic C–H carbon signals for the para substituted aromatic ring are easily distinguishable and observed at δ 115 and 122. The methyl (Ar–CH_3) and methyleneoxy (–OCH_2) carbon signlas are observed at δ 16 and 65 respectively and methoxy (–OCH_3) carbon signal is found at δ 56.0.

The mass spectra of newly prepared C_3 symmetric tris-imines showed mass peaks corresponding to $(M+Na)^+$ in accordance with their proposed structures as base peak using mass spectrometer having TOF mass analyzer with ES technique except for compound **32b** (-Br substituted; Spectrum 16) and compound **32c** (-NO_2 substituted; Spectrum 36). Elemental analysis results supported the proposed structures.

6.2.3 Host-guest study of compounds 32 with I transition series metal ions

For the expanded tris-imino compounds having the binding imino hydroxyl sites placed remotely compare to the earlier tripodal hosts, host-guest binding study was carried out with I transition metal ion perchlorate salts by using UV-vis and fluorescence spectroscopy as a visualizing tools.

Binding of these host molecules with Fe^{3+} ions was visible with development of colour different from the host solution resulting into a new absorption band between 500 to 600 nm which was not observed in the presence of the other transition metal ions (Figure 24, Graphs 23-26 and inset figures).

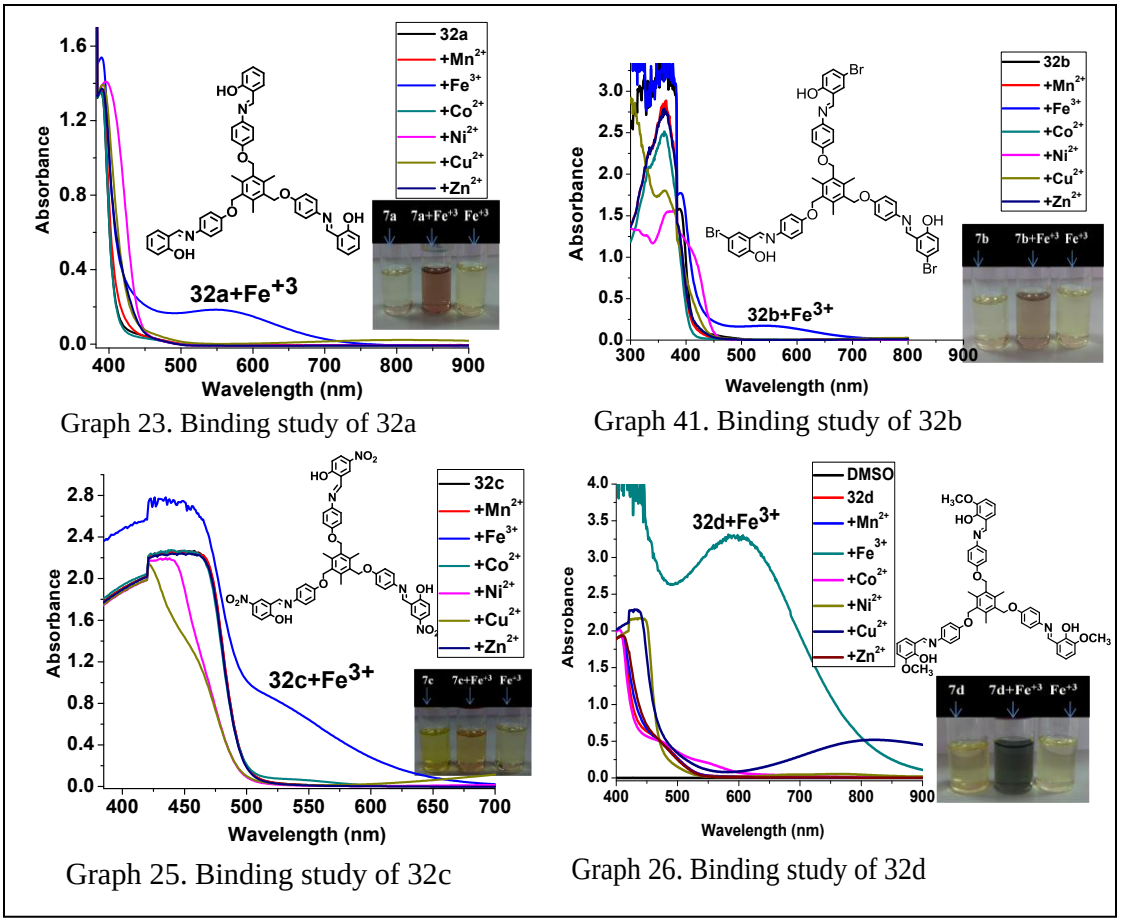

Graph 23. Binding study of 32a

Graph 41. Binding study of 32b

Graph 25. Binding study of 32c

Graph 26. Binding study of 32d

Figure 24 (Graph 23-26) ***UV-Vis spectra assisted binding study of compounds 32a-e with I series transition metal ions***

The selectivity study between Fe^{3+} and other metal ions using UV-vis spectroscopy showed that the present host molecules were not as selective as the earlier ones for Fe^{3+} (Figure 25, Graph 27-31).

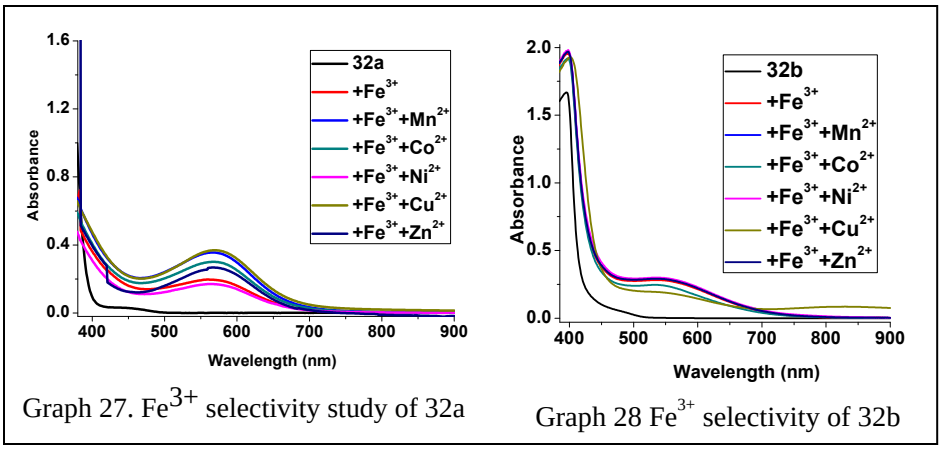

Graph 27. Fe^{3+} selectivity study of 32a

Graph 28 Fe^{3+} selectivity of 32b

Figure 25 ***UV-vis spectra of Fe^{3+} selectivity for 32a-b*** *contined..*

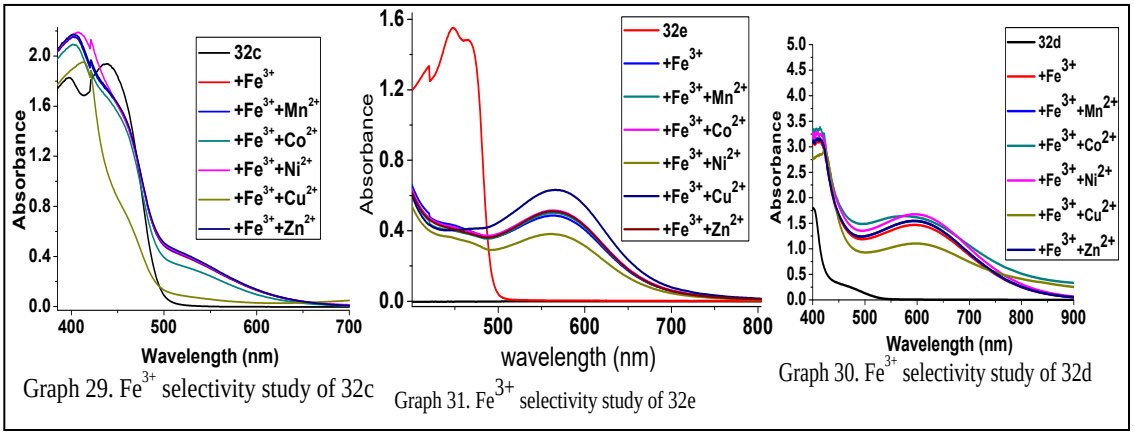

Graph 29. Fe^{3+} selectivity study of 32c

Graph 31. Fe^{3+} selectivity study of 32e

Graph 30. Fe^{3+} selectivity study of 32d

Figure 25 ***UV-vis spectra of Fe^{3+} selectivity in presence of other metal ions for 32a-e***

The hosts **32b** and **32d**with bromo and methoxy substituents (Figure 25, Graph 28 and 30) had greater selectivity for Fe^{3+} compared to the other analogues hosts.

The stoichiometry of hosts binding with Fe^{3+} ions studied by Jobs method was showing host : guest in 1:1 ratio except for the host **32c** (Figure 26).

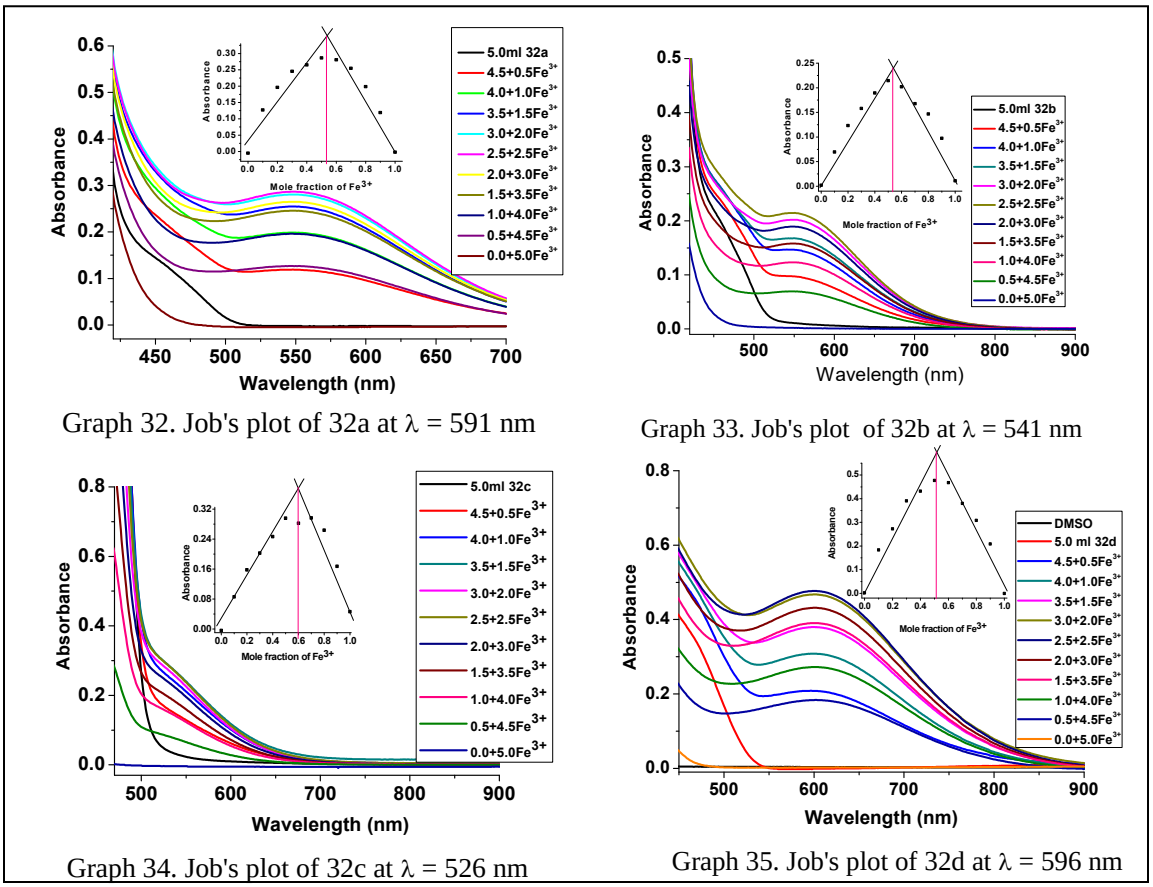

Graph 32. Job's plot of 32a at λ = 591 nm

Graph 33. Job's plot of 32b at λ = 541 nm

Graph 34. Job's plot of 32c at λ = 526 nm

Graph 35. Job's plot of 32d at λ = 596 nm

Figure 26 ***Job's plot for compounds 32a-e***

Fluorescence spectroscopy was also useful to study binding of transition metal ions with C_3 symmetric tripodal imines. It also helped in studying selectivity between transition metal ions under photoluminescence conditions. The hydroxyl imine tripodal host without further substitution **32a** (Figure 27, Graph 36), with bromo substitution **32b** (Figure 27, Graph 37)and with methoxy substitution **32d** (Figure 27, Graph 38)when excited at 420 nm showed emission near 500 nm with varying intensities with lowest intensity emission band for **32a**. Fluorescence was getting totally off in the presence of Fe^{3+}, Cu^{2+} and Ni^{2+} guest ions (Figure 27).

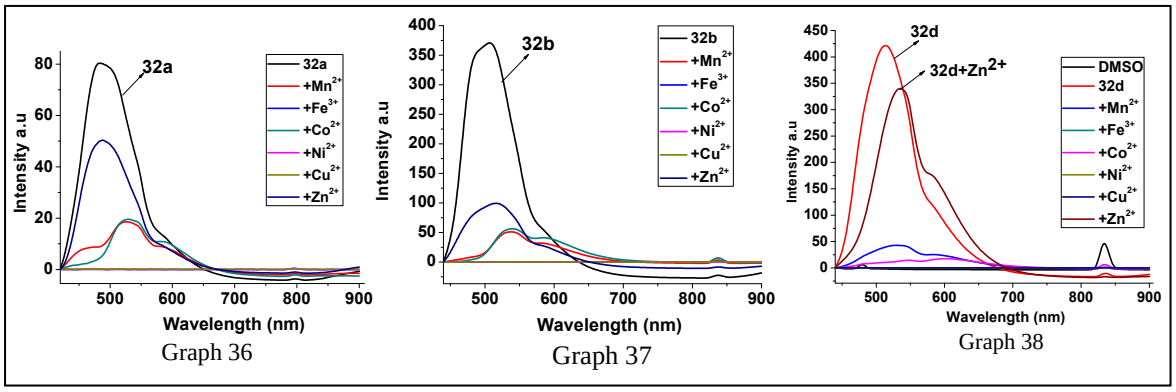

Graph 36 Graph 37 Graph 38

Figure 27 ***Binding study using fluorescence for hosts 32a, 32b and 32d***

Fe^{3+} selectivity study was carried for the latter two compounds **32b** and **32d** having greater fluorescence. Fe^{3+} was turning off fluorescence of the host molecules even in the presence of other metal ions also (Figure 28, Graph 39 - 40).

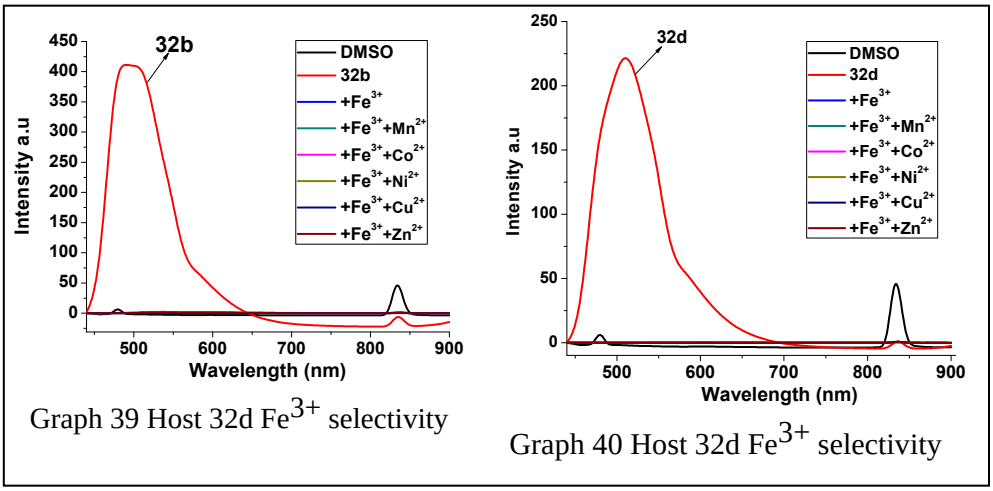

Graph 39 Host 32d Fe^{3+} selectivity Graph 40 Host 32d Fe^{3+} selectivity

Figure 28 ***Fluorescence monitored Fe^{3+} selectivity study for hosts 32b and 32d***

For nitro substituted tripodal host compound **32c**, Cu^{2+} and Ni^{2+} had greater effect on fluorescence intensity compared to the other transition metal ions. In this case, Ni^{2+} was making fluorescence totally off (Figure 29, Graph 41). Selectivity study conducted, showed that fluorescence reduction was influenced by Fe^{3+} ions even when the other metal ions were present with the interference of these metal ions as seen in the figure 29, Graph 42.

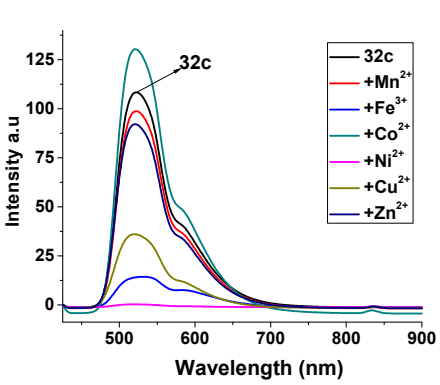

Graph 41 Binding study host 32c

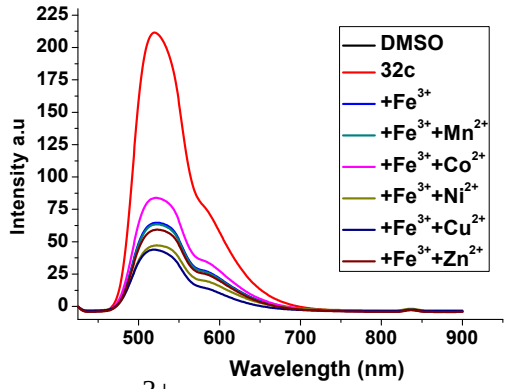

Graph 42 Fe^{3+} Selectivity study of host 32c

Figure 29 ***Fluorescence assisted binding and selectivity study for 32c***

The tripodal α-hydroxynapthyl imine compound **32e** when studied for its role as a host molecule in presence of I row transition metal ions using UV-Vis spectroscopy showed a prominent colour change in the presence of Fe^{3+} with absorption band near λ_{max} 600 nm in DMSO as a solvent. The other metal ions had no significant influence on UV-vis spectrum of the host molecule in the visible region (Figure 30, Graph 43).

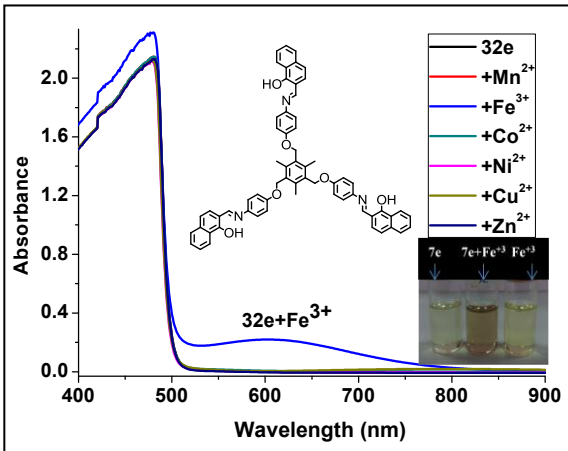

Graph 43 Binding study of 32e

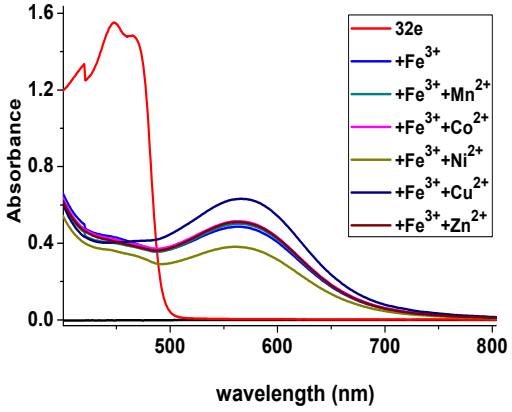

Graph 44. Fe^{3+} selectivity study of 32e

Figure 30 ***Transition metals binding and selectivity study for 32e using UV-vis tool***

Selectivity study carried out for Fe^{3+} in the presence of other metal ions showed that the host molecule was selectively binding with Fe^{3+} with development of colour as well a new absorption band (Figure 30, Graph 44). Thus the host can be used as colorimetric sensor for Fe^{3+} ions even in the presence of other metal ions.

The host guest stoichiometry was found to be 1:1 as observed from Job's plot (Figure 31, Graph 45). It indicated that all the three podands were involved in binding with the guest entity.

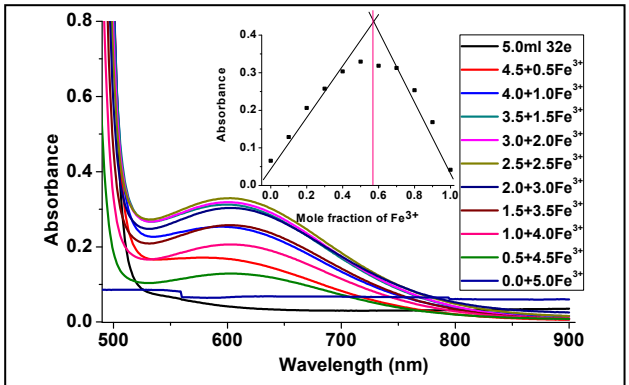

Graph 45. Jobs's plot at λ = 602 nm

Figure 31 ***Job's plot for 32e***

Photoluminescence study was carried out for **32e** with excitation λ = 420 nm, showed a weak emission band for the host molecule at λ = 506 nm. Emission band was influenced, with enhancement in fluorescence intensity in presence of Fe^{3+} while fluorescence was quenched in presence of Cu^{2+}, the other metal ions had no or little influence on the fluorescence of the host molecule (Figure 32, Graph 46).

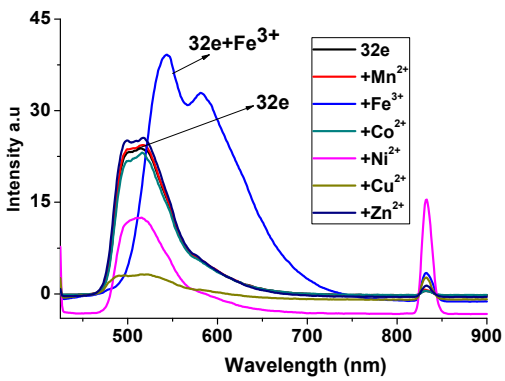

Graph 46. Binding study of 32e

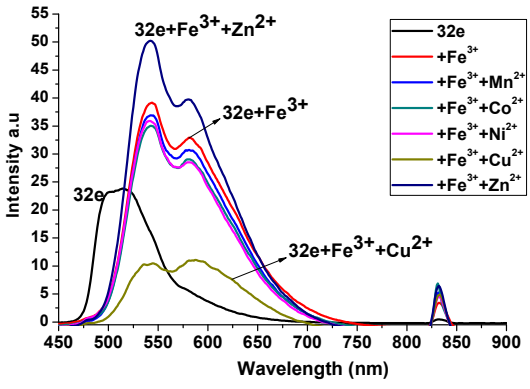

Graph 47. Fe^{3+} selectivity study of 32e

Figure 32 ***Fluorescence study of 32e and transition metal ions***

The selectivity study was carried out for Fe^{3+} in the presence of other metal ions. It was observed that the host selectively bound with Fe^{3+} resulting in an enhancement in fluorescence except in presence of Cu^{2+}, thus Cu^{2+} was found to interfere binding of the host molecule with Fe^{3+} (Figure 32, Graph 47).

Binding study of the same host molecule was reported in HEPES buffer (4-(2-hydroxyethyl)-1-piperazineethanesulfonic acid) solution with a variety of metal ions including the transition metal ions, It was found to act as a selective fluorescence sensor for Al^{3+} and Pb^{2+} with fluorescence being turned on.[26] Contrary to the reported study, the present study was carried out in DMSO wherein Fe^{3+} was not included in the previous study.

6.3 CONCLUSION

Two types of C_3 symmetric tris-imino compounds were synthesized with hydroxyl-imino binding sites. In the first series of compounds, the chelating sites were nearer to the central aromatic ring and also nearer to each other while in the second series analogous compounds prepared with aryloxy space group had the imino functionality moving farther from each other and away from the central aromatic ring. The tripodal compounds were found to be good colorimetric Fe^{3+} sensors and in some cases fluorescence spectroscopy also led to the same conclusion. Host compounds without aromatic spacer were found to be good host and colorimetric sensors as studied using UV-vis spectroscopy. For the host even with spacer, the imino-hydroxyl binding sites were participating in binding with the guest ions and were selective in few cases (–Br and $–OCH_3$). In general, the presence of nitro group in the tripodal host molecules showed interference of Cu^{2+} when selectivity study was carried out for Fe^{3+}. The presence of methoxy substitution in both the types of tripodal hosts showed greater selectivity towards Fe^{3+} colorimetrically. The tripodal host with hydroxy napthyl imino functionality was found as a good host without spacer in comparison to with spacer colorimetrically but were non-fluorescent. Photoluminescence study of hosts with electron releasing substitutions such as –Br and $–OCH_3$ showed greater fluorescence and in the presence of Fe^{3+}, Cu^{2+} and Ni^{2+} ions fluorescence was getting off except for host with spacer and nitro substitution. Selectivity study for Fe^{3+} in presence of the other metal ions showed quenching of fluorescence without any interference.

6.4 EXPERIMENTAL

6.4.1 1,3,5–Tris(aminomethyl)–2,4,6–trimethylbenzene[25] 27:

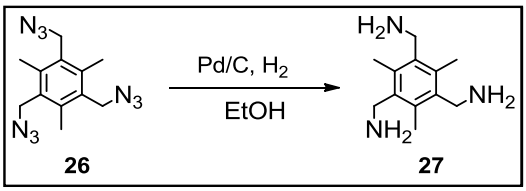

In a round bottom flask (50 ml) was placed 1,3,5-trisazidomehtyl-2,4,6-trimewthylbenzene **26** (2.0 g 1.0 mmol) in absolute ethanol (EtOH) and Pd/C (5 mol% (0.5 g) and reaction was stirred at room temperature under H_2 atmosphere with positive pressure for 14 hours. The reaction mixture was filtered through celite and solvent was evaporated under vacuum to give the white crystalline solid. Product was used further without purification for the next reaction. Yield 93%; **IR:** 3360, 3290, 2912, 1594, 1451, 1374, 1375, 1104 cm^{-1}; mp. 64–65 °C (*Lit.* 66 °C).[27]

6.4.2 1,3,5-Tris[(2-hydroxyarylidene)-aminomethyl]-2,4,6-trimethylbenzenes 29:

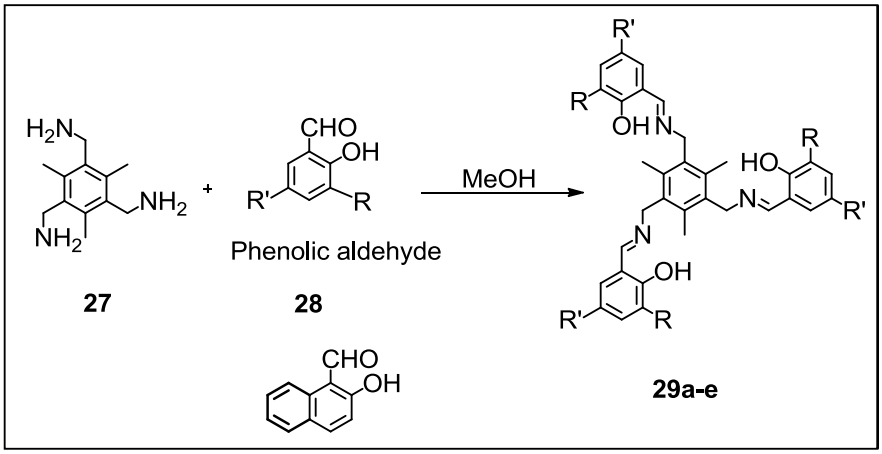

To a solution of **27** (0.5 g, 2.42 mmol) in methanol was added dropwise methanolic solution of appropriate phenolic aldehyde **28** (7.5 mmol) at room temperature. After the addition, the reaction mixture was allowed to stir for 1-2 hours resulting into precipitation of the products. In some cases yellow precipitation was formed immediately upon addition. The residue was filtered and dried under vacuum. The crude product obtained was purified by recrystallization from ethanol.

1,3,5–Tris[(2–hydroxyarylidene)–aminomethyl]–2,4,6–trimethylbenzene (29a)

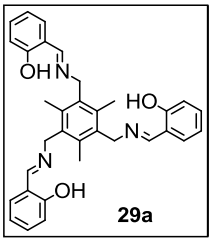

29a

29a was prepared from **27** (0.5 g, 2.42 mmol) and 2-hydroxybenzaldehyde **28a** (0.8 ml, 7.5 mmol) following the general procedure described above as a yellow solid. Yield: 0.86 g, 75%; mp: 190 °C.

IR (KBr) : 2868, 1628, 1581, 1495, 1278, 755 cm^{-1}; **^{1}H NMR ($CDCl_3$) :** δ (ppm) 2.41 (9H, s, $–CH_3$), 4.98 (6H, s, $–NCH_2–$), 6.84-6.88 (3H, dt, J_{ortho} = 15.0 Hz), 6.94-6.96 (3H, d, J = 8.0 Hz), 7.22-7.24 (3H, dd, J = 7.6 Hz), 7.28-7.32 (3H, dt, J_{ortho} = 14.8 Hz), 8.27 (3H, s, –N=CH), 13.50 (3H, s, –OH); **^{13}C NMR :** δ (ppm) 16.3 ($–CH_3$), 56.6 ($–OCH_2–$), 116.9, 118.5, 118.9, 131.4, 132.2, 132.4, 137.1, 160.9 (Ar-OH), 164.3 (–N=CH); **Mass (TOF MS ES+):** *m/z* calculated for $C_{33}H_{33}N_3O_3$: 519.2522, found: (*m/z*) 520.2337 $(M+H)^+$, 542.2126 (100%, $(M+Na))^+$; **Elemental analysis :** Calculated for $C_{33}H_{33}N_3O_3$: C 76.28%, H 6.40%, N 8.09%, found: C 75.97%, H 6.37%, N 7.85%.

1,3,5–Tris[5–bromo–(2–hydroxyarylidene)–aminomethyl]–2,4,6–trimethylbenzene (29b)

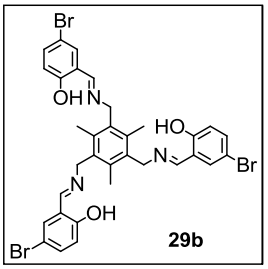

29b

29b was prepared from **27** (0.5 g, 2.42 mmol) and 5-bromo-2-hydroxybenzaldehyde **28b** (1.5 g, 7.5 mmol) following the general procedure described as a yellow solid. Yield: 1.0 g, 60%; mp: 253 °C.

IR (KBr) : 3449, 1631, 1571, 1476, 1359, 1279, 1198, 818, 625 cm^{-1}; **^{1}H NMR ($CDCl_3$) :** δ (ppm) 2.38 (9H, s, $–CH_3$), 4.99-5.00 (6H, d, J = 1.2 Hz $–NCH_2$), 6.85-6.87 (3H, dt, J = 8.4 Hz), 7.35-7.37 (3H, dd, J = 5.6 Hz), 7.39 (3H, d, J = 2.4 Hz), 8.18 (3H, s, –N=CH), 13.48 (3H, s, –OH); **^{13}C NMR :** δ (ppm) 16.3 ($–CH_3$), 56.5 ($–OCH_2–$), 96.1 (C-Br), 110.0, 119.0, 120.2, 132.2, 133.5, 134.9, 137.2, 160.0 (Ar-OH), 163.2 (–N=CH); **Mass (TOF MS ES+):** calculated for $C_{33}H_{30}Br_3N_3O_3$ 752.9837 *m/z*, found (*m/z*) 701.4998 100% $(M–3OH)^+$; **Elemental analysis:** Calculated for $C_{33}H_{30}Br_3N_3O_3$: C 52.41%, H 4.00%, N 5.56%, found: C 52.15%, H 4.24%, N 5.33%.

1,3,5–Tris[5–nitro–(2–hydroxyarylidene)–aminomethyl]–2,4,6–trimethylbenzene (29c)

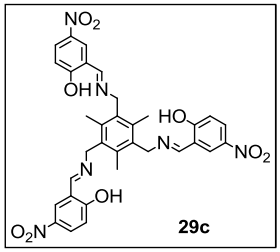

29c was prepared from **27** (0.5 g, 2.42 mmol) and 5-nitro-2-hydroxybenzaldehyde **28c** (1.25 g, 7.5 mmol) following the general procedure as a bright yellow solid. Yield: 1.14 g, 72%; mp: 247 °C.

IR (KBr) : 3431, 3060, 2910, 1644, 1608, 1547, 1337, 1227, 1096 cm^{-1}; **^{1}H NMR (DMSO-*d6*) :** δ (ppm) 2.46 (9H, s, $–CH_3$), 5.06 (6H, s, $–NCH_2–$), 6.72-6.75 (6H, d, J = 9.6 Hz), 8.06-8.09 (3H, dd, J = 9.4 Hz), 8.48-8.49 (3H, d, J = 3.2 Hz), 8.76 (3H, s, –N=CH); **^{13}C NMR (DMSO-*d6*) :** δ (ppm) 16.5 ($–CH_3$), 52.7 ($–OCH_2–$), 115.8, 121.3, 129.1, 131.2, 131.8, 136.3, 138.4, 166.1 (–N=CH), 174.0 (Ar-OH); **Mass (TOF MS ES+):** *m/z* calculated for $C_{33}H_{30}N_6O_9$ 654.2074, found (*m/z*) 636.97 $(M–H_2O)^+$, 542.91 100% $(M–H_2O–NO_2)^+$; **Elemental analysis:** Calculated for $C_{33}H_{30}N_6O_9$: C 60.55%, H 4.62%, N 12.84%, found: C 59.79%, H 4.70%, N 12.79%.

1,3,5-Tris[3-methoxy-(2-hydroxyarylidene)-aminomethyl]-2,4,6-trimethylbenzene (29d)

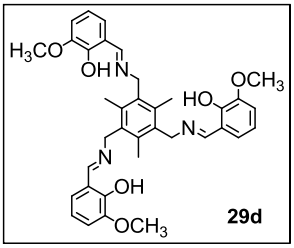

29d was prepared from **27** (0.5 g, 2.42 mmol) and 2-hydroxy-3-methoxy benzaldehyde **28d** (1.13 g, 7.5 mmol) following the general procedure described as a yellow solid. Yield: 0.57 g, 42%; mp: 163 °C.

IR (KBr) : 3052, 2992, 2918, 2849, 1632, 1471, 1251, 1079 cm^{-1}; **^{1}H NMR ($CDCl_3$) :** δ (ppm) 2.42 (9H, s, $–CH_3$), 3.90 (9H, s, $–OCH_3$), 4.97 (6H, s, $–NCH_2–$), 6.77-6.81 (3H, t), 6.85-6.87 (3H, dd, J = 8.0 Hz), 6.09-6.92 (13H, dd, J = 7.8 Hz), 8.26 (3H, s, –N=CH), 14.02 (3H, s, –OH); **^{13}C NMR :** δ (ppm) 16.3 ($–CH_3$), 56.1 ($–OCH_2–$), 56.3, 113.9, 117.8, 118.6, 123.1, 132.4, 137.0, 1448.4, 151.6 (Ar-OH), 164.3 (–N=CH); **Mass (TOF MS ES+):** *m/z* calculated for $C_{36}H_{39}N_3O_6$: 609.2839, found: (*m/z*) 632.2446 (100%, M+Na) $^+$; **Elemental analysis: C**alculated for $C_{36}H_{39}N_3O_6$: C 70.92%, H 6.45%, N 6.89%, found: C 70.96%, H 6.37%, N 6.66%.

1,3,5–Tris[(2–hydroxynapthylidene)–aminomethyl]–2,4,6–trimethylbenzene (29e)

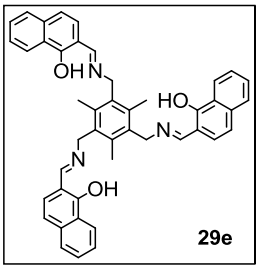

29e was prepared from **27** (0.5 g, 2.42 mmol) and 2-hydroxy-1-napthaldehyde **28e** (1.3 g, 7.5 mmol) following the procedure described as a yellow solid. Yield: 1.02 g, 70%; mp: 258 °C.

IR (KBr) : 3408, 1631, 1544, 1355, 1292, 1211 cm^{-1}; **^{1}H NMR ($CDCl_3$) :** δ (ppm) 2.58 (9H, s, $–CH_3$), 5.01 (6H, s, $–NCH_2–$), 6.96-6.98 (3H, d, J = 9.2 Hz), 7.21-7.25 (3H, dt, J_{ortho} = 14.8 Hz), 7.33-7.37 (3H, dt, J_{ortho} = 15.4 Hz), 7.63-7.65 (3H, dd, J = 7.6 Hz), 7.70-7.72 (3H, d, J = 9.2 Hz), 7.78-7.80 (3H, dd, J = 8.4 Hz), 8.88 (3H, s, –N=CH), 14.98 (3H, s, –OH); **^{13}C NMR :** δ (ppm) 16.6 ($–CH_3$), 52.4 ($–OCH_2–$), 107.4, 118.1, 122.9, 123.7, 126.6, 127.9, 129.2, 132.1, 133.2, 136.5, 137.6, 157.9 (–N=CH), 172.5 (Ar-OH); **Mass (TOF MS ES+):** *m/z* calculated for $C_{45}H_{39}N_3O_3$ 669.2991, found: (*m/z*) 692.2561 (100%, M+Na) $^+$; **Elemental analysis: C**alculated for $C_{45}H_{39}N_3O_3$: C 80.69%, H 5.87%, N 6.27%; found: C 80.60%, H 5.67%, N 6.11%.

6.4.2 1,3,5–Tris(4–aminophenyloxymethyl)–2,4,6–trimethylbenzene[26] 31:

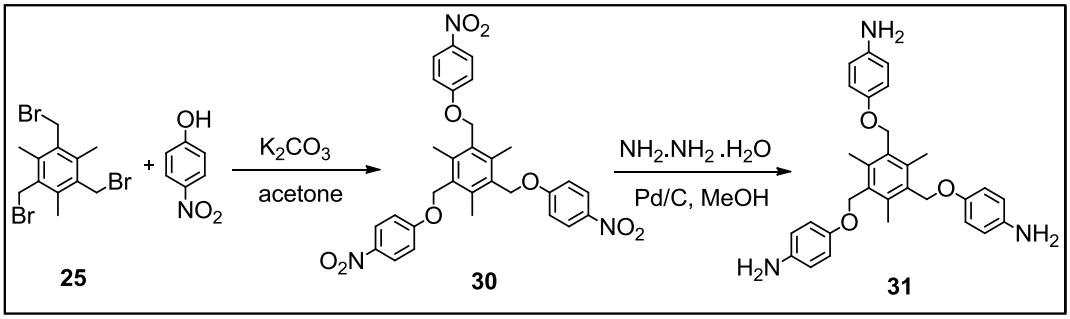

To a stirred solution of 4-nitrophenol (1.0 g, 7.6 mmol), and K_2CO_3 (3.2 g, 22.5 mmol) in acetone was added tris-bromomethyl mesitylene **25** (1.0 g, 2.5 mmol) and the mixture was allowed to stir at room temperature for 3 hours. After the completion of the reaction, acetone was evaporated under reduced pressure and water was poured into the flask. White solid separated out was filtered under suction and was dried. Resulting product **30** obtained was used for the next step without purification. Yield: 1.4 g, 96%; **^{1}H NMR:** δ

(ppm) 2.47 (9H, s, $–CH_3$), 5.23 (6H, s, $–OCH_2–$), 7.09–7.11 (6H, d, J = 9.2 Hz), 8.27–8.29 (6H, d, J = 9.2 Hz); mp. 212–214 °C (*Lit.* 215 °C).[26]

Compound **30** (0.5 g, 0.87 mmol) in methanol (15-20 ml) was mixed with 99% hydrazine hydrate ($NH_2.NH_2.H_2O$, 2.5 ml) and the reaction mixture was degassed and then Pd/C 5% (0.17 g) was added. The resulting mixture was refluxed for 12 hours. After completion of the reaction, reaction mixture was filtered through celite and washed with MeOH, solvent was evaporated under reduced pressure and residue was washed with water to yield the desired compound **31** which was used further without purification. Yield 0.32 g, 77%; **^{1}H NMR:** δ (ppm) 2.44 (9H, s, $–CH_3$), 5.01 (6H, s, $–OCH_2–$), 5.99 (6H, s, $–NH_2$) 6.86–6.70 (6H, d, J = 8.4 Hz), 6.86–6.88 (6H, d, J = 8.4 Hz); mp. 170-172 °C (*Lit.* 172 °C).[26]

6.4.5 1,3,5–Tris[4–(2–hydroxyarylidene–amino)–phenyloxymethyl]–2,4,6–trimethyl-benzene 32:

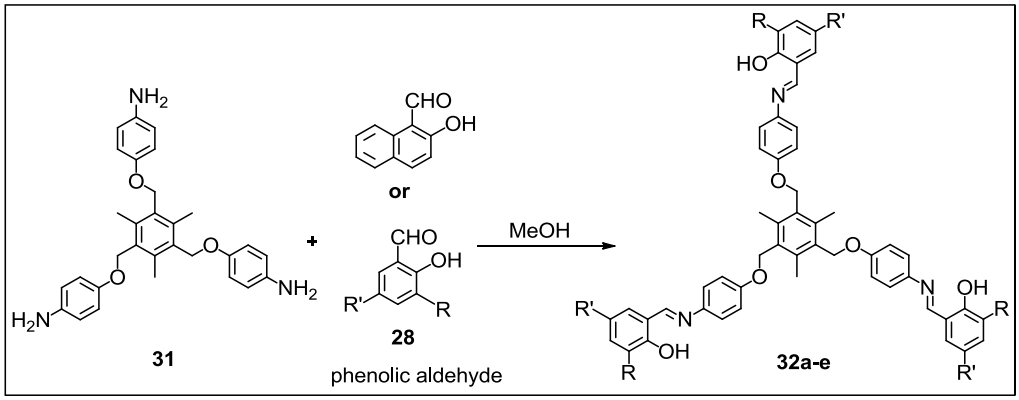

Tris(imino) compounds **32** were synthesized by known method. To a solution of **31** 1.0 mmol in methanol was added dropwise methanolic solution of appropriate phenolic aldehyde **28** 3.1 mmol at 50 °C. After complete addition, reaction mixture was refluxed for 1-2 hours resulting into precipitation. In some cases yellow precipitation was formed immediately upon addition. Reaction mixture was cooled, filtered and the crude was dried under vacuum. Residue was purified by recrystallization technique using ethanol as a solvent.

1,3,5–Tris[4–(2–hydroxyarylidene–amino)–phenyloxymethyl]–2,4,6–trimethyl-benzene (32a)

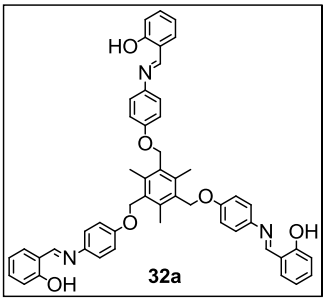

32a

32a was prepared from **31** (0.5 g, 2.42 mmol) and 2-hydroxybenzaldehyde **28a** (0.34 ml, 7.5 mmol) following the general procedure as a yellow solid. Yield: 0.52 g, 63%; mp: 182 °C.

IR (KBr) : 3435, 3038, 2984, 2903, 1616, 1507, 1281, 1233, 1187 cm^{-1}; **^{1}H NMR ($CDCl_3$) :** δ (ppm) 2.50 (9H, s, $–CH_3$), 5.17 (6H, s, $–OCH_2–$), 6.94-6.98 (3H, dt, J_{ortho} = 15.0 Hz), 7.03-7.05 (3H, d, J = 8.0 Hz), 7.09-7.11 (6H, dd, J = 6.8 Hz), 7.33-7.36 (6H, dd, J = 6.8 Hz), 7.38-7.42 (6H, dt, J_{ortho} = 13.8 Hz), 8.65 (3H, s, –N=CH), 13.46 (3H, s, –OH); **^{13}C NMR :** δ (ppm) 16.0 ($–CH_3$) , 65.2 ($–OCH_2–$), 115.3, 117.1, 119.0, 119.3, 122.4, 131.6, 132.0, 132.7, 139.4, 141.7, 158.3 (Ar-O), 160.6 (–N=CH), 160.9 (Ar-OH); **Mass (TOF MS ES+):** *m/z* calculated for $C_{51}H_{45}N_3O_6$: 795.3308, found: (*m/z*) 818.2853 (100%, M+Na) $^+$; **Elemental analysis:** Calculated for $C_{51}H_{45}N_3O_6$: C 79.96%, H 5.70%, N 5.28%, found: C 79.60%, H 5.68%, N 5.17%.

1,3,5–Tris[4–{5–bromo–(2–hydroxyarylidene–amino)}–phenyloxymethyl]–2,4,6–tri-methylbenzene (32b)

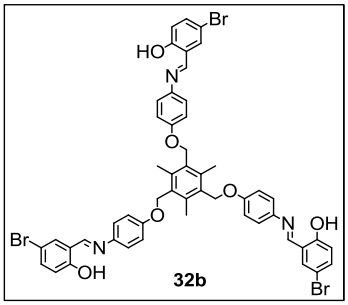

32b

32b was prepared from **31** (0.5 g, 2.42 mmol) and 5-bromo-2-hydroxybenzaldehyde **28b** (0.54 g, 7.5 mmol) following the general procedure described as an orange solid. Yield: 0.73 g, 68%; mp: 210 °C.

IR (KBr) : 3435, 2915, 1617, 1500, 1475, 1276, 1233, 1175, 991, 821, 625 cm^{-1}; **^{1}H NMR ($CDCl_3$) :** δ (ppm) 2.50 (9H, s, $–CH_3$), 5.17 (6H, s, $–OCH_2–$), 6.92-6.94 (3H, d, J = 8.8 Hz), 7.09-7.11 (6H, dd, J_{ortho} = 7.2 Hz), 7.32-7.34 (6H, dd, J_{ortho} = 6.8 Hz), 7.43-7.46 (3H, dd, J = 8.8 Hz), 7.51 (3H, d, J = 2.4 Hz), 8.56 (3H, s, –N=CH), 13.43 (3H, s, –OH); **^{13}C NMR :** δ (ppm) 16.0 ($–CH_3$), 65.3 ($–OCH_2–$), 96.1, 110.4, 115.4, 119.1, 120.7, 122.5, 131.6, 133.9, 135.3, 139.4, 141.1, 158.6 (Ar-O), 159.0 (–N=CH), 160.0 (Ar-OH); **Mass (TOF MS ES+):** *m/z* calculated for $C_{51}H_{42}Br_3N_3O_6$: 1029.0624, found

(*m/z*) 701.5052 100%; **Elemental analysis: C**alculated for $C_{51}H_{42}Br_3N_3O_6$: C 59.32%, H 4.10%, N 4.07%, C 59.96%, H 4.22%, N 3.92%.

1,3,5–Tris[4–{5–nitro–(2–hydroxyarylidene–amino)}–phenyloxymethyl]–2,4,6–tri–methylbenzene (32c)

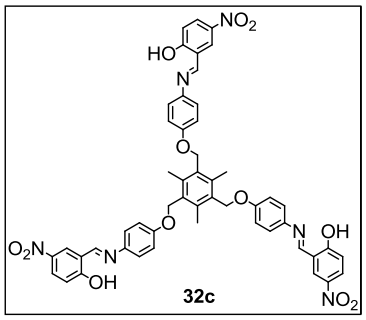

32c

32c was prepared from **31** (0.5 g, 2.42 mmol) and 5-nitro-2-hydroxybenzaldehyde **28c** (0.56 g, 7.5 mmol) following the general procedure described as a bright yellow solid. Yield: 0.65 g, 67%; mp: 240 °C.

IR (KBr) : 3634, 3068, 2905, 1620, 1485, 1338, 1295, 1235, 1094, 827 cm^{-1}; **^{1}H NMR (DMSO-*d6*) :** δ (ppm) 2.40 (9H, s, $–CH_3$), 5.20 (6H, s, $–OCH_2–$), 7.08-7.10 (3H, d, J = 9.2 Hz), 7.20-7.23 (6H, d, J = 9.2 Hz), 7.53-7.55 (6H, d, J = 8.8 Hz), 8.22-8.25 (3H, dd, J = 9.2 Hz), 8.63-8.64 (3H, d, J = 2.8 Hz), 9.17 (3H, s, –N=CH); **^{13}C NMR (DMSO-*d6*) :** δ (ppm) 16.0 ($–CH_3$) , 65.7 ($–OCH_2–$), 116.0, 118.8, 118.9, 123.3, 128.5, 128.8, 131.8, 139.4, 139.6, 159.2 (Ar-O), 159.9 (–N=CH), 167.5 (Ar-OH); **Mass (TOF MS ES+):** *m/z* calculated for $C_{51}H_{42}N_6O_{12}$: 930.2861, found (*m/z*) 636.93 100%; **Elemental analysis:** Calculated for $C_{51}H_{42}N_6O_{12}$: C 65.8%, H 4.55%, N 9.03%, C 64.91%, H 4.75%, N 8.56%.

1,3,5–Tris[4–{6–methoxy–(2–hydroxyarylidene–amino)}–phenyloxymethyl]–2,4,6–trimethylbenzene (32d)

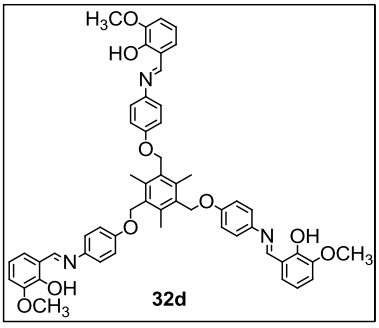

32d

32d was prepared from **31** (0.5 g, 2.42 mmol) and 3-methoxy-2-hydroxybenzaldehyde **28d** (0.49 g, 7.5 mmol) following the general procedure described as an orange solid. Yield: 0.81 g, 90%; mp: 155 °C.

IR (KBr) : 3435, 2933, 1616, 1505, 1464, 1254, 980 cm^{-1}; **^{1}H NMR ($CDCl_3$) :** δ (ppm) 2.50 (9H, s, $–CH_3$), 3.96 (9H, s, $–OCH_3$), 5.16 (6H, s, $–OCH_2–$), 6.88-6.92 (3H, t), 6.99-7.01 (1H, dd, J = 8.0 Hz), 7.03-7.05 (3H, dd, J = 7.8 Hz), 7.08-7.12 (6H, m, J_{ortho} = 7.8

Hz), 7.33-7.35 (6H, m, J_{ortho} = 6.8 Hz), 8.65 (3H, s, –N=CH), 13.9 (3H, s –OH); **^{13}C NMR :** δ (ppm) 16.0 (–CH_3), 56.1 (–OCH_3), 65.2 (–OCH_2), 114.3, 115.3, 118.4, 119.2, 122.4, 123.5, 131.6, 139.4, 141.3, 148.4, 151.2, 158.3 (Ar-O), 160.5 (–N=CH), 163.4 (Ar-OH); **Mass (TOF MS ES+):** *m/z* calculated for $C_{54}H_{41}N_3O_9$: 885.3625, found: (*m/z*) 908.3173 (100%, M+Na)$^+$; **Elemental analysis: C**alculated for $C_{54}H_{41}N_3O_9$: C 73.2%, H 5.80%, N 4.74%, C 72.99%, H 5.75%, N 4.61%.

1,3,5–Tris[4–(2–hydroxynapthylidene–amino)–phenyloxymethyl]–2,4,6–trimethyl-benzene (32e)[26]

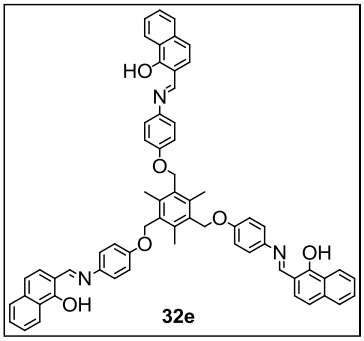

32e

32e was prepared from **31** (0.5 g, 2.42 mmol) and 2-hydroxy-1-napthaldehyde **28e** (0.56 g, 7.5 mmol) following the general procedure described as an orange solid. Yield: 0.85 g, 87%; mp: 110 °C.

IR (KBr) : 1620, 1501, 1235, 1173, 996 cm^{-1}; **^{1}H NMR (DMSO-*d6*) :** δ (ppm) 2.42 (9H, s, –CH_3), 5.19 (6H, s, –OCH_2), 7.02-7.04 (3H, d, *J* = 9.2 Hz), 7.21-7.23 (6H, d, *J* = 8.8 Hz), 7.33-7.37 (3H, t), 7.53-7.56 (3H, t), 7.66-7.69 (6H, d, *J* = 8.8 Hz), 7.79-7.81 (3H, d, = 8.0 Hz), 7.90-7.93 (3H, d, *J* = 9.2 Hz), 9.66-9.67 (3H, d, *J* = 4.4 Hz, –N=CH), 16.03-16.04 (3H, d, *J* = 4.4 Hz, –OH).

6.5 SPECTRAL DATA

Compound 27

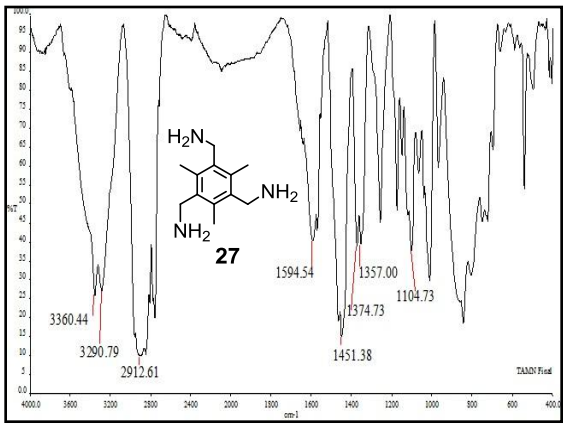

Spectrum 1. IR of 27

Compound 29a

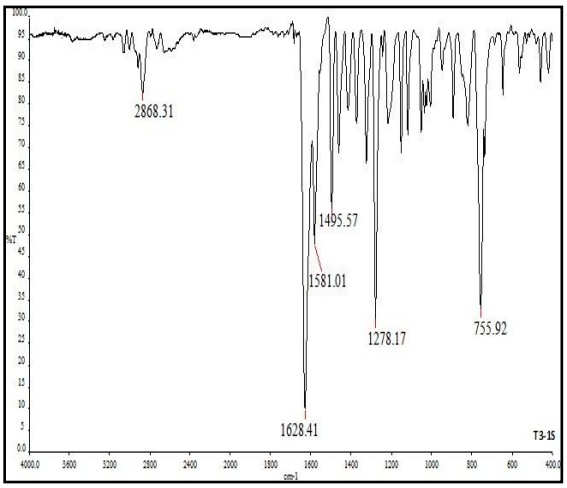

Spectrum 2. IR of 29a

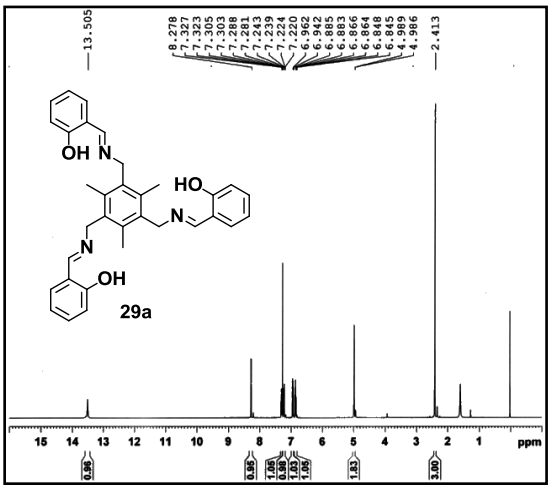

Spectrum 3. ^{1}H NMR of 29a

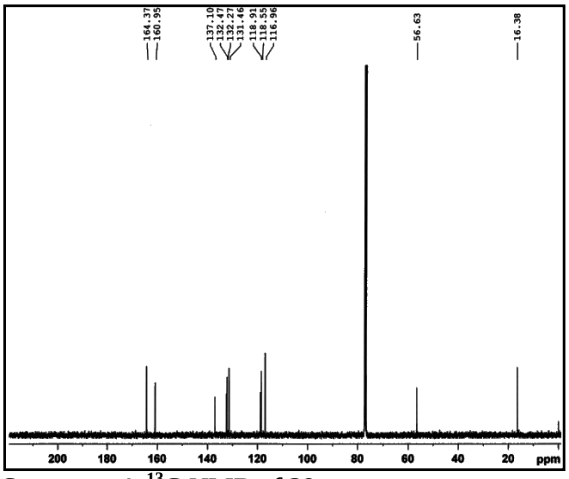

Spectrum 4. ^{13}C NMR of 29a

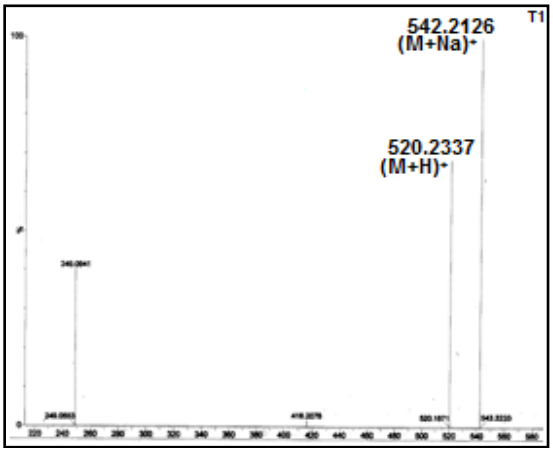

Spectrum 5. Mass of 29a

Compound 29b

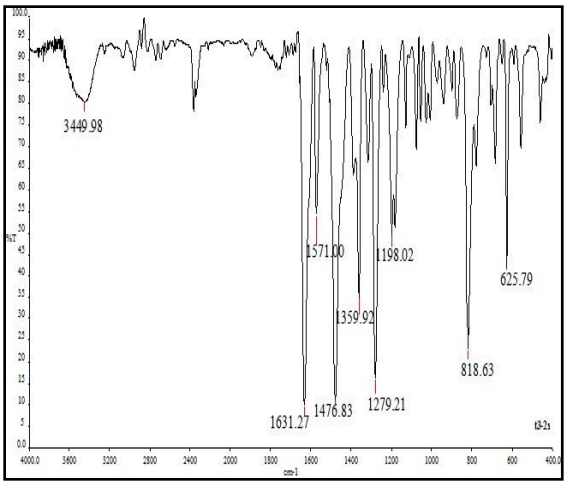

Spectrum 6. IR of 29b

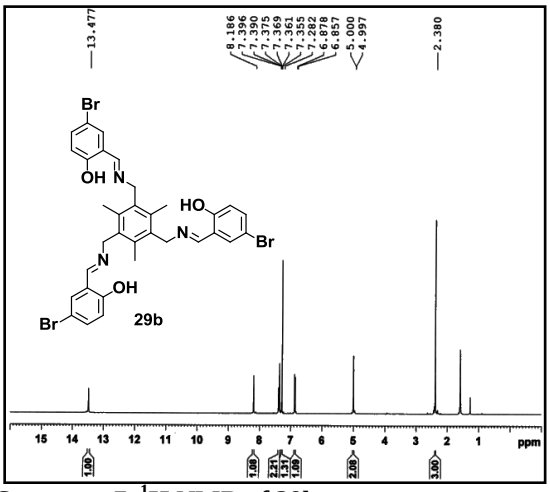

Spectrum 7. ^{1}H NMR of 29b

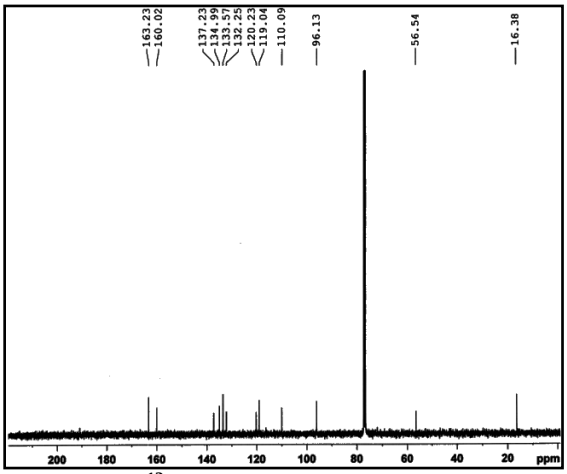

Spectrum 8. ^{13}C NMR of 29b

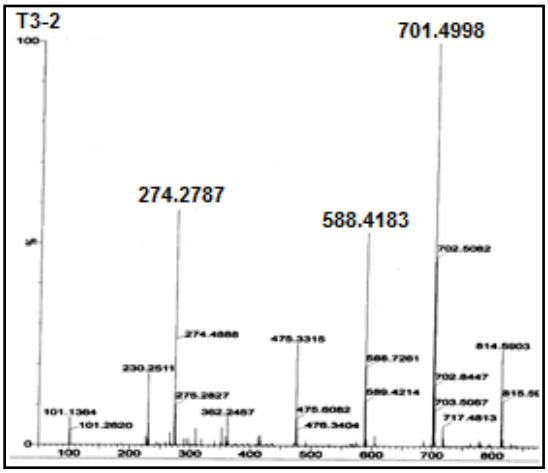

Spectrum 9. Mass of 29b

Compound 29c

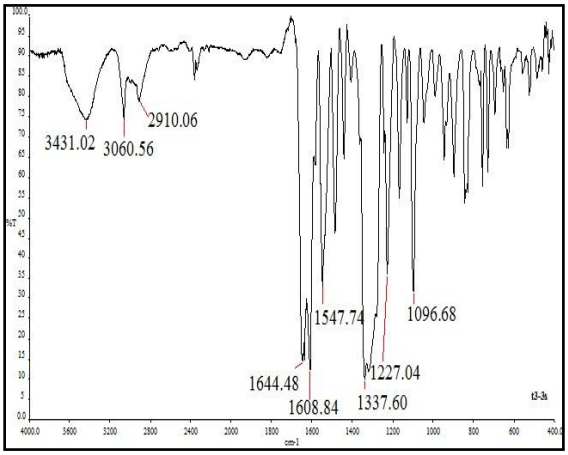

Spectrum 10. IR of 29c

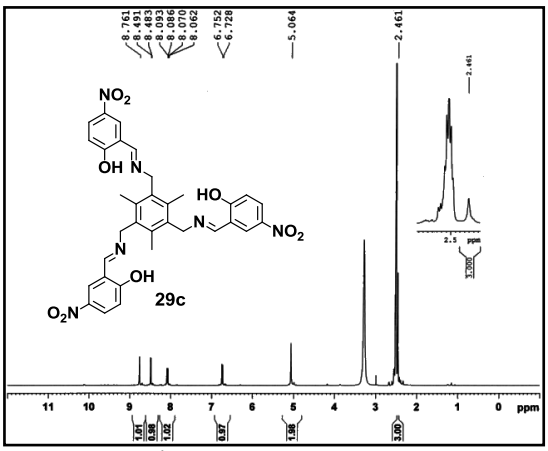

Spectrum 11. ^{1}H NMR of 29c

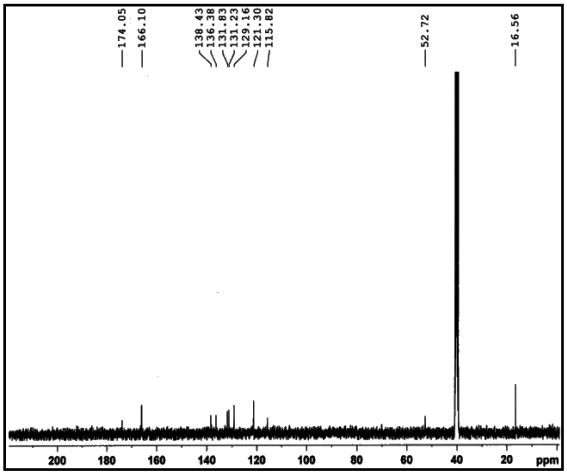

Spectrum 12. ^{13}C NMR of 29c

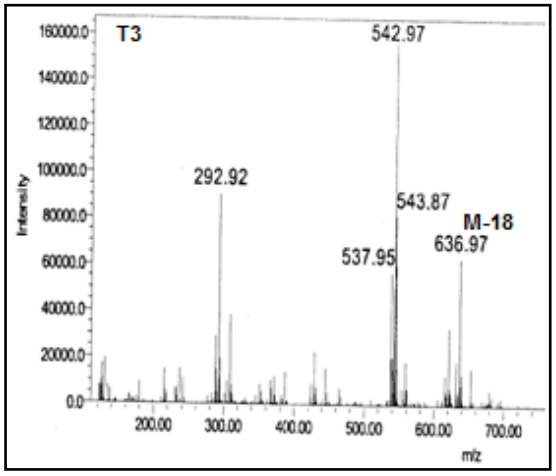

Spectrum 13. Mass of 29c

Compound 29d

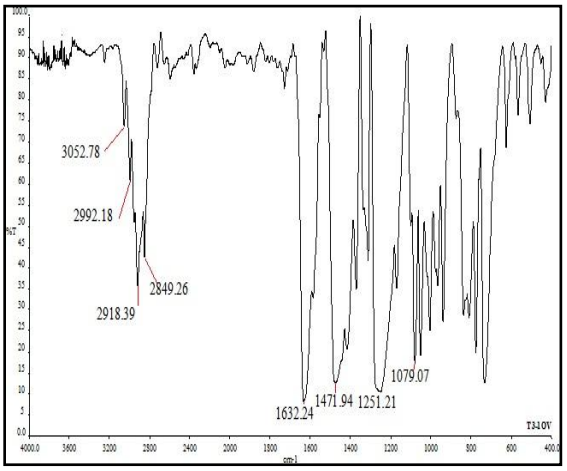

Spectrum 14. IR of 29d

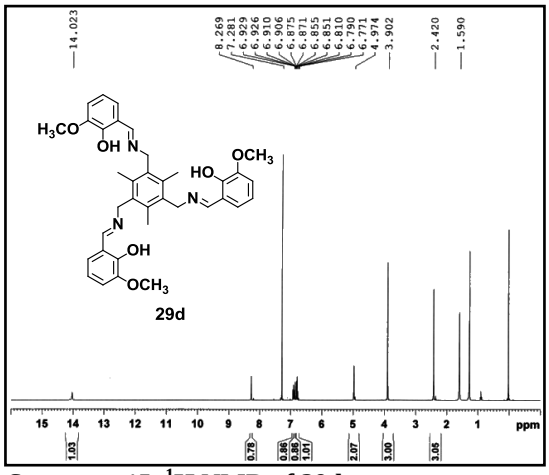

Spectrum 15. ^{1}H NMR of 29d

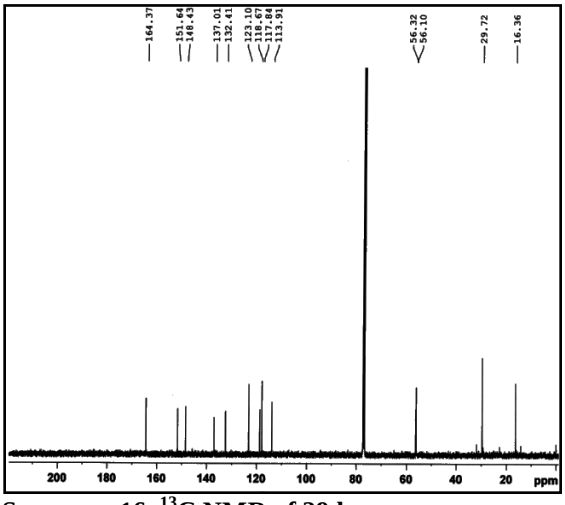

Spectrum 16. ^{13}C NMR of 29d

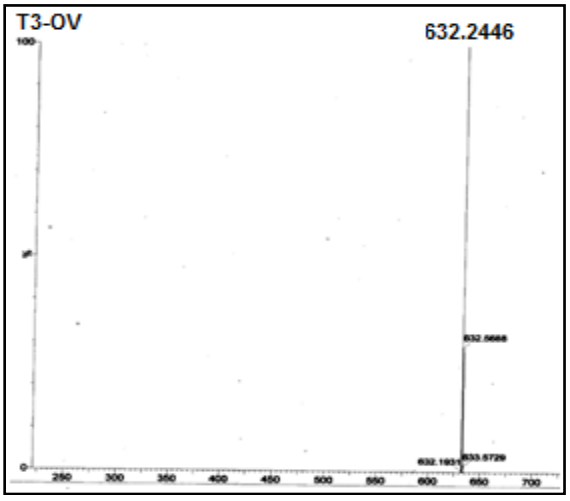

Spectrum 17. Mass of 29d

Compound 29e

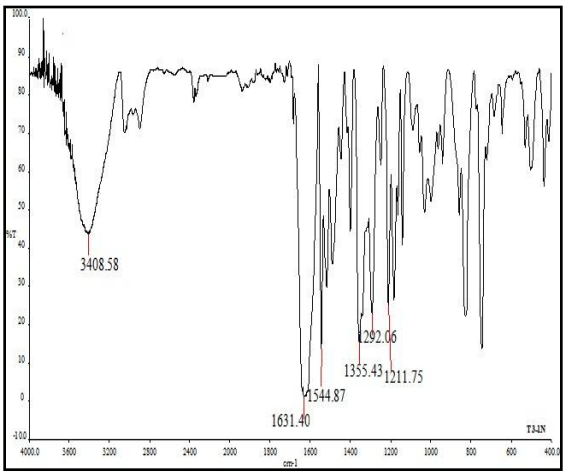

Spectrum 18. IR of 29e

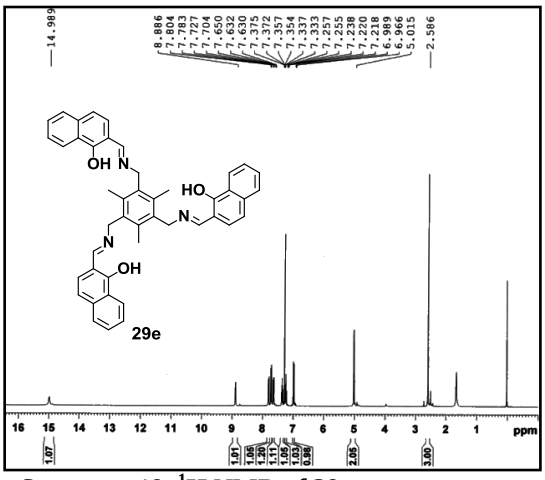

Spectrum 19. ^{1}H NMR of 29e

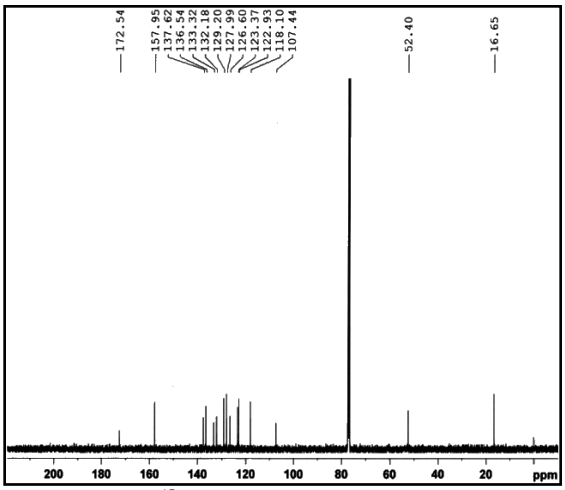

Spectrum 20. ^{13}C NMR of 29e

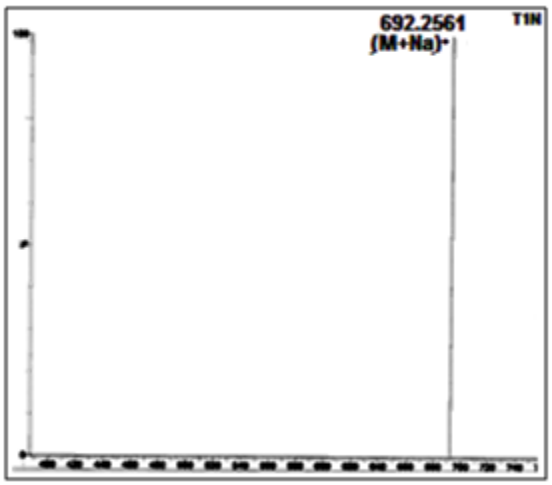

Spectrum 21. Mass of 29e

Compound 30

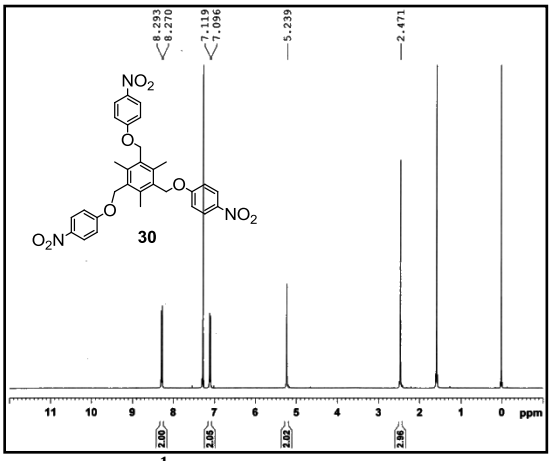

Spectrum 22. ^{1}H NMR of 30

Compound 31

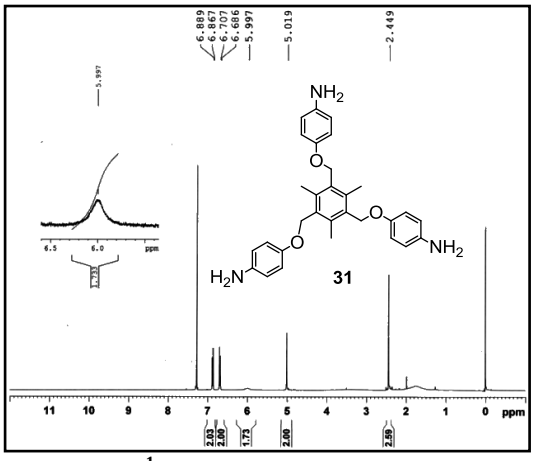

Spectrum 23. ^{1}H NMR of 31

Compound 32a

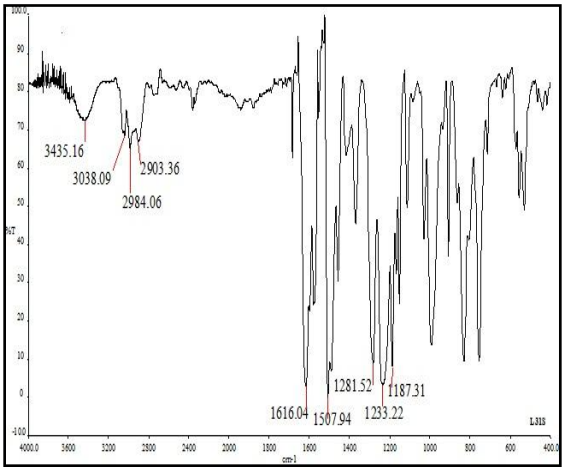

Spectrum 24. IR of 32a

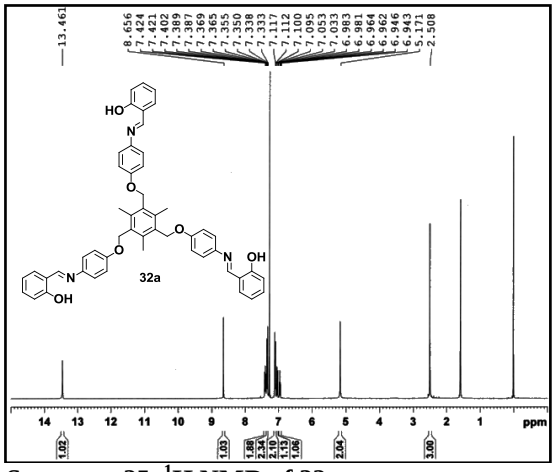

Spectrum 25. ^{1}H NMR of 32a

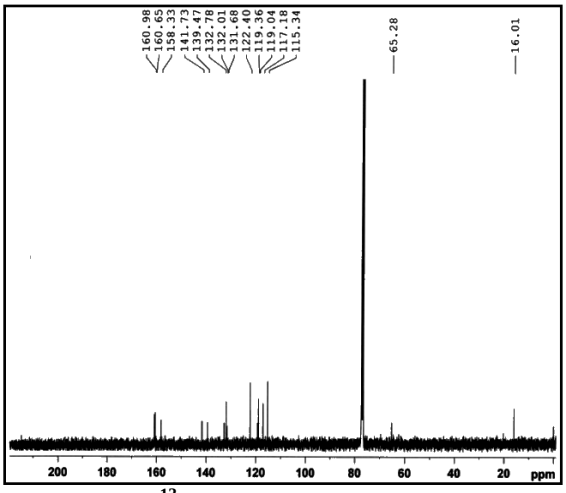

Spectrum 26. ^{13}C NMR of 32a

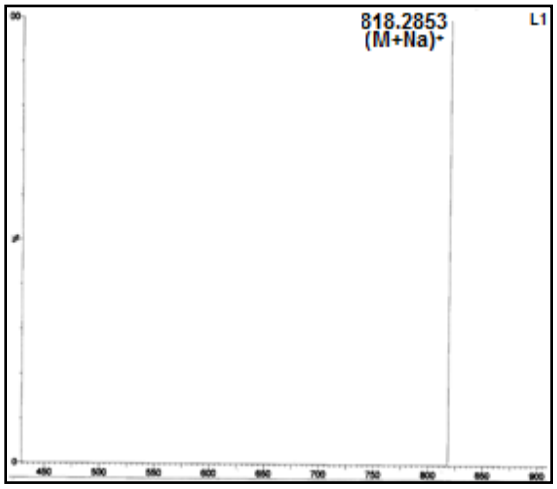

Spectrum 27. Mass of 32a

Compound 32b

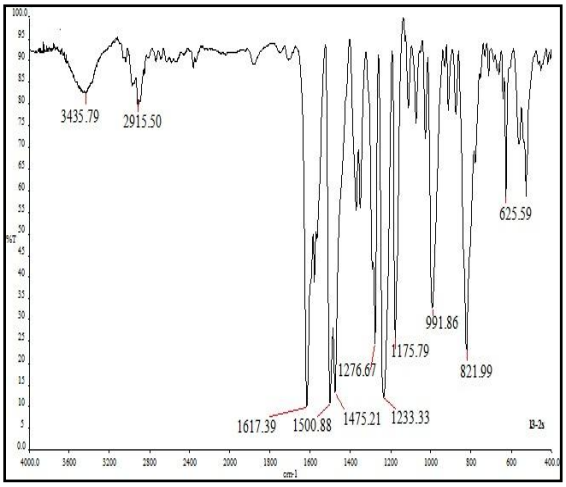

Spectrum 28. IR of 32b

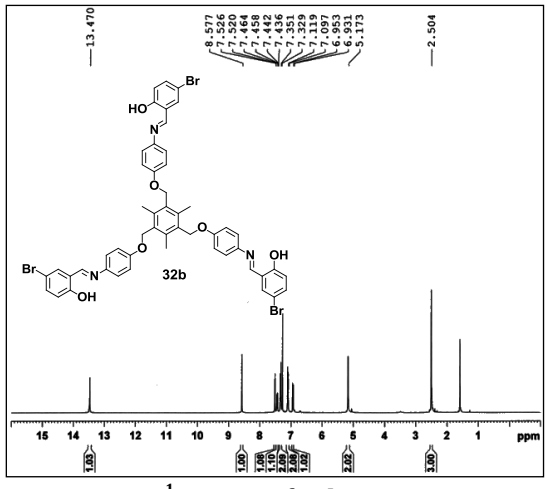

Spectrum 29. ^{1}H NMR of 32b

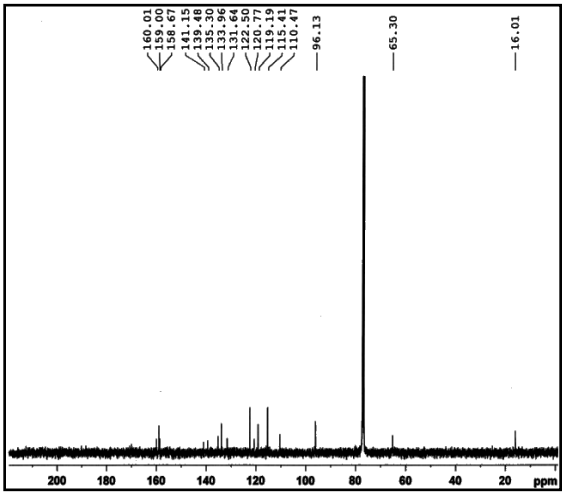

Spectrum 30. ^{13}C NMR of 32b

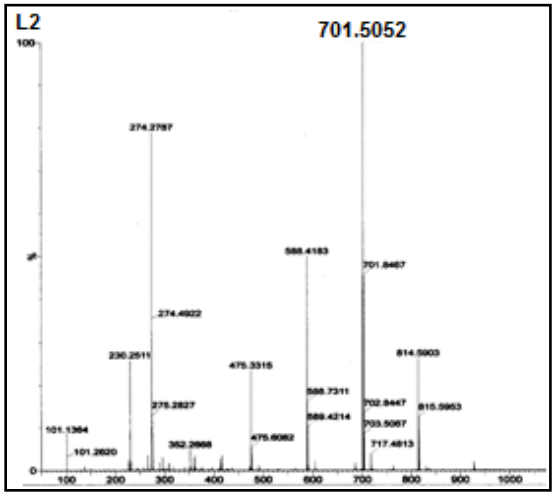

Spectrum 31. Mass of compound 32b

Compound 32c

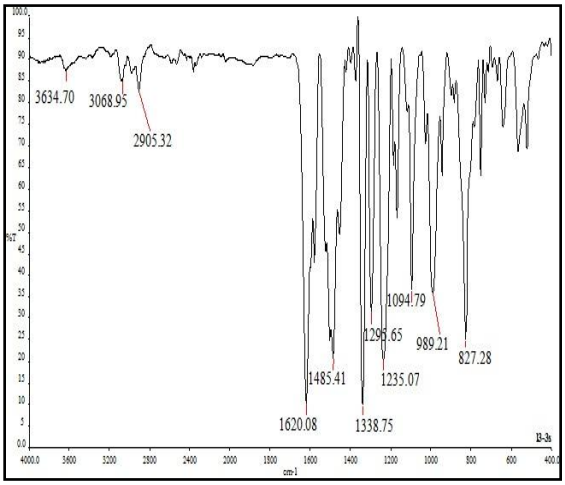

Spectrum 32. IR of 32c

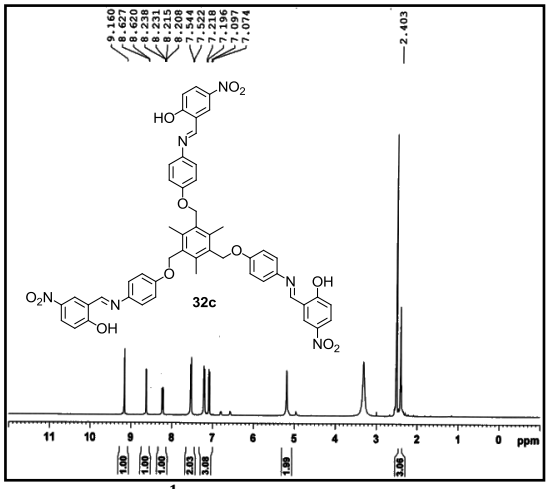

Spectrum 33. ^{1}H NMR of 32c

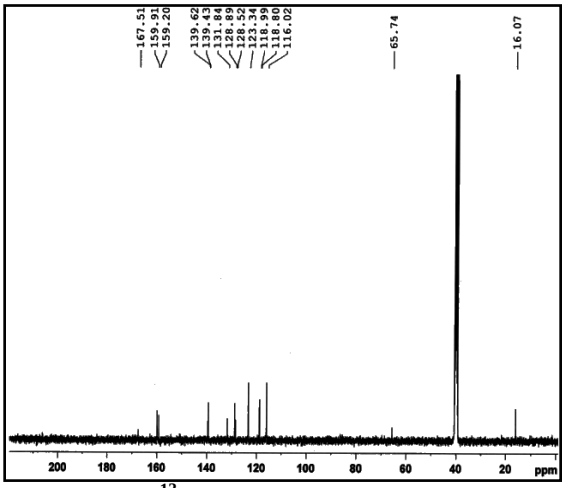

Spectrum 34. ^{13}C NMR of 32c

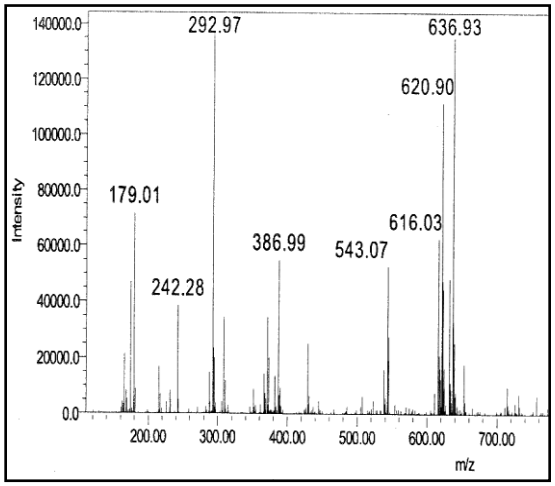

Spectrum 35. Mass of 32c

Compound 32d

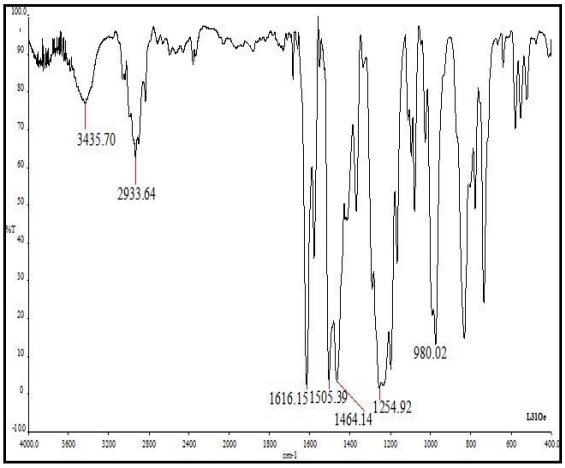

Spectrum 36. IR of 32d

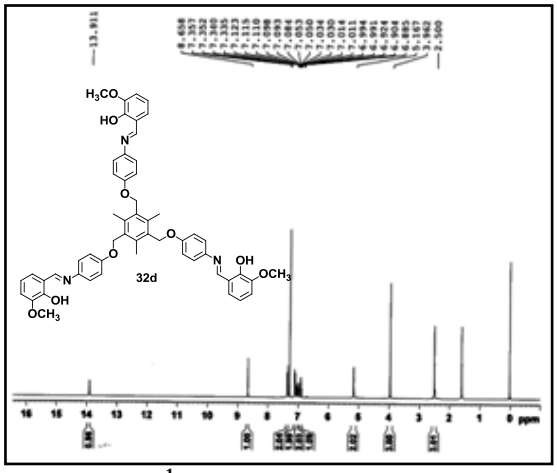

Spectrum 37. ^{1}H NMR of 32d

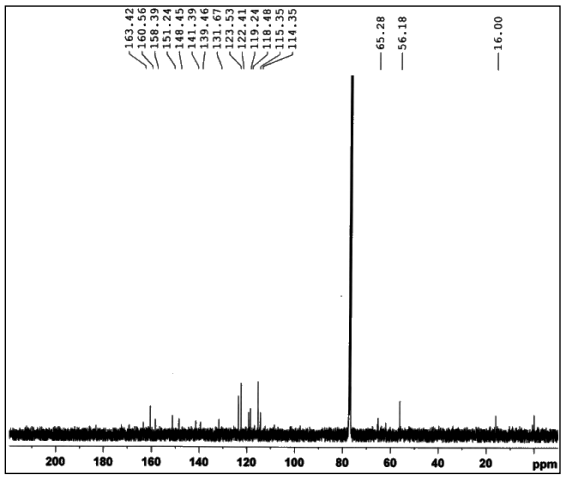

Spectrum 38. ^{13}C NMR of 32d

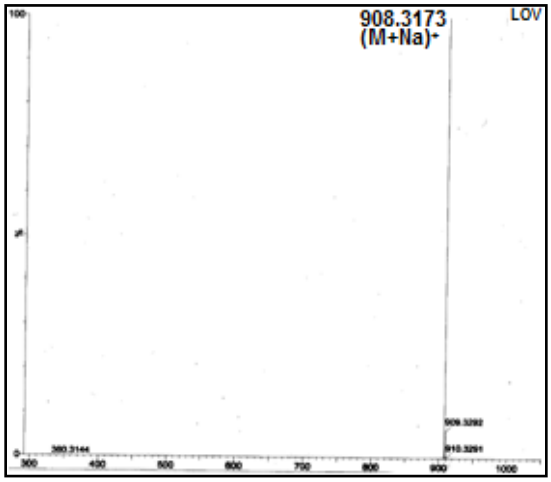

Spectrum 39. Mass of 32d

Compound 32e

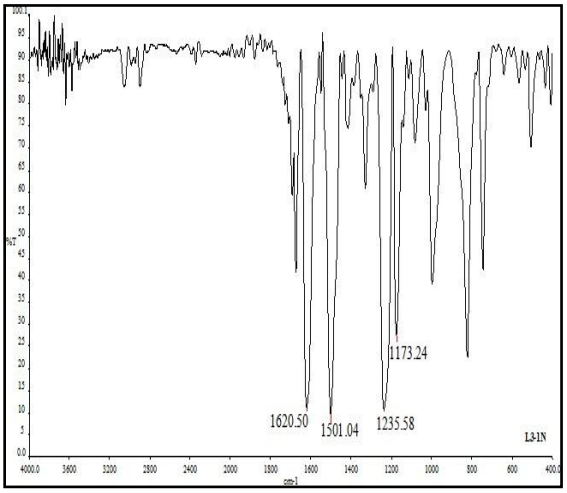

Spectrum 40. IR of 32e

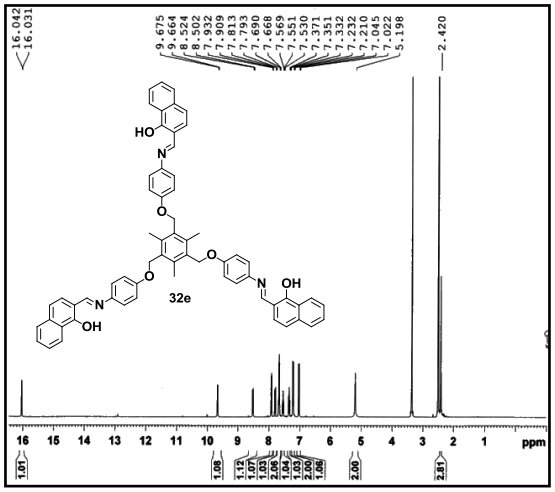

Spectrum 41. ^{1}H NMR of 32e

REFERENCES

1. Qin, W.; Long, S.; Panunzio, M.; Biondi, S. *Molecules* **2013**, *18*, 12264–12289.
2. Buonora, P.; Olsen, J. C.; Oh, T. *Tetrahedron* **2001**, *57*, 6099–6138.
3. (a) Dhawan, R.; Arndtsen, B. A. *J. Am. Chem. Soc.* **2004**, *126*, 468–469 (b) Kel'in, A. V.; Sormek, A. W.; Gevorgyan, V. *J. Am. Chem. Soc.* **2001**, *123*, 2074–2075.
4. Colby, D. A.; Bergman, R. G.; Ellman, J. A. *J. Am. Chem. Soc.* **2008**, *130*, 3645–3651.
5. St. Cyr, D. J.; Martin, N.; Arndtsen, B. A. *Org. Lett.* **2007**, *9*, 449–452.
6. Zhang, Y. R.; He, L.; Wu, X.; Shao, P. L.; Ye, Song *Org. Lett.* **2008**, *10*, 277–280.
7. Siamaki, A. R.; Arndtsen, B. A. *J. Am. Chem. Soc.* **2006**, *128*, 6050–6051.
8. (a) Yamada, K.; Tomioka, K. *Chem. Rev.* **2008**, *108*, 2874–2886; (b) Yey, L. *Angew. Chem. Int. Ed.* **2001**, *40*, 875–877; (c) Kobayashi, S.; Ishitani, H. *Chem. Rev.* **1999**, *99*, 1069–1094; (d) Dai, L-X.; Lin, Y-R.; Hou, X-L.; Zhou, Y-G. *Pure Appl. Chem.* **1999**, *71*, 1033–1040.
9. (a) M. S. Iyer, K. M. Gigstad, N. D. Namdev, M. Lipton, *J. Am. Chem. Soc*. **1996**, *118*, 4910–4911; (b) M. S. Iyer, K. M. Gigstad, N. D. Namdev, M. Lipton, *Amino Acids* **1996**, *11*, 259–268.
10. Porter, J. R. Traverse, J. F.; Hoveyda, A. H.; Snapper, M. L. *J. Am. Chem. Soc.* **2001**, *123*, 984–985.
11. Cozzi, P. G. *Chem. Soc. Rev.* **2004**, *33*, 410–421.
12. Whiteoak, C. J.; Salassa, G.; Kleij, A. W. *Chem. Soc. Rev.* **2012**, *41*, 622–631.
13. Chatterjee, A.; Bennur, T. H.; Joshi, N. N. *J. Org. Chem.* **2003**, *68*, 5668–5671.
14. Shi, L.; Ge, H. M.; Tan, S. H.; Li, H. Q.; Song, Y. C.; Zhu, H. L.; Tan, R. X. *Eur. J. Med. Chem.* **2007**, *42*, 558–564.
15. Mohsen, M. K.; Ali, H. I.; Anwar, M. M. *Eur. J. Med. Chem.* **2010**, *45*, 572–580.
16. Sondhi, S.; Singh, N.; Kumar, A.; Lozache, O.; Meijer, L. *Biorg. & Med. Chem.* **2006**, *14*, 3578–3581.
17. (a) Kajal, A.; Bala, S.; Kamboj, S.; Sahrma, N.; Saini, V. *Journal of Catalysts* **2013**, 1–14; (b) Anand, P.; Patil, V. M.; Sharma, V. K.; Khosa, R. L.; Masand, L. *International Journal of Drug Design and Discovery* **2012**, *3*, 851–868; (c) Arulmurugan, S.; Kavitha, H. P; Venkatraman, B. R. *RASAYAN J. Chem.* **2010**, *3*,

385–410; (d) Simplicio, A. L.; Clancy, J. M.; Gilmer, J. F. *Molecules* **2008**, *13*, 519–547.

18. (a) Hsieh, W. H.; Wan, C-F.; Liao, D-J.; Wu, A-T. *Tetrahedron Lett.* **2012**, *53*, 5848–5851; (b) Zhou, X-X.; Cai, Y-P.; Zhu, S-Z.; Zhan, Q-G.; Liu, M-S.; Zhou, Z-Y.; Chen, L. *Crystal Growth & Design* **2008**, *8*, 2076–2079; (c) Bhattacharya, P.; Parr, J.; Ross, A. T.; Slawin, A. M. Z. *J. Chem. Soc. Dalton Trans.* **1998**, 3149–3150.
19. (a) Kanungo, B. K.; Baral, M.; Sahoo, S. K.; Muthu, S. E. *Spectrochimica Acta Part A* **2009**, *74*, 544–552; (b) Kanungo, B. K.; Sahoo, S. K.; Baral, M. *Spectrochimica Acta Part A* **2008**, *71*, 1452–1460.
20. (a) Bharadwaj, V. K.; Hundal, M. S.; Hundal, G. *Tetrahedron* **2009**, *65*, 8556–8562; (b) Suresh, P.; Srimurugan, S.; Babu, B.; Pati, H. N. *Tetrahedron: Asymmetry* **2007**, *18*, 2820–2827; (c) Singh, N.; Hundal, M. S.; Hundal, G.; Martinez-R.; M. *Tetrahedron* **2005**, *61*, 7796–7806; (d) Singh, N.; Kumar, M.; Hundal, G. *Inorganica Chimica Acta* **2004**, *357*, 4286–4290.
21. Sharma, S.; Hundal, M. S.; Singh, N.; Hundal, G. *Sensors and Actuators B* **2013**, *188*, 590–596.
22. Bhardwaj, V. K.; Pannu, A.; Singh, N.; Hundal, M.; Hundal, G. *Tetrahedron* **2008**, *64*, 5384–5391.
23. Bhardwaj, V. K.; Singh, N.; Hundal, M. S.; Hundal, G. *Tetrahedron* **2006**, *62*, 7878–7886.
24. Katritzky, A. R.; Singh, S. K.; Meher, N. K.; Doskocz, J.; Suzuki, K.; Jiang, R.; Sommen, G. L.; Ciaramitaro, D. A.; Steel, P. J. A*RKIVOC* **2006**, 43–62.
25. Carrero, P.; Ardá, A.; Alvarez, M.; Doyagüez, E. G.; Rivero-Buceta, E.; Quesada, E.; Prieto, A.; Solís, D.; Camarasa, M. J.; Peréz-Pérez, M. J.; Jiménez-Barbero, J.; San-Félix, A. *Eur. J. Org. Chem.* **2013**, 65–76.
26. Datta, B. K.; Kar, C.; Basu, A.; Das, G. *Tetrahedron Lett.* **2013**, *54*, 771–774.